

Carbonate fluxes by coccolithophore species between NW Africa and the Caribbean: Implications for the biological carbon pump

Catarina V. Guerreiro^{1,2*}, Karl-Heinz Baumann^{3,4}, Geert-Jan A. Brummer⁵, André Valente¹,
Gerhard Fischer^{3,4}, Patrizia Ziveri^{6,7}, Vanda Brotas^{1,8}, Jan-Berend W. Stuut^{5,9}

¹MARE, Marine and Environmental Sciences Centre, Faculty of Sciences of the University of Lisbon, Lisbon, Portugal

²IDL, Instituto Dom Luiz, Faculty of Sciences of the University of Lisbon, Lisbon, Portugal

³Department of Geosciences, University of Bremen, Bremen, Germany

⁴MARUM, Center for Marine and Environmental Sciences, University of Bremen, Bremen, Germany

⁵Department of Ocean Systems, NIOZ Royal Netherlands Institute for Sea Research, Den Burg, The Netherlands

⁶ICREA, Catalan Institution for Research and Advanced Studies, Barcelona, Spain

⁷ICTA-UAB, Institut de Ciència i Tecnologia Ambientals—Universitat Autònoma de Barcelona, Barcelona, Spain

⁸Department of Plant Biology, Faculty of Sciences of the University of Lisbon, Lisbon, Portugal

⁹Faculty of Earth and Life Sciences, VU Vrije Universiteit, Amsterdam, The Netherlands

Abstract

Coccolithophores are among the most important calcifying pelagic organisms. To assess how coccolithophore species with different coccolith-carbonate mass and distinct ecological resilience to ocean warming will influence the “rain ratio” and the “biological carbon pump”, 1 yr of species-specific coccolith-carbonate export fluxes were quantified using sediment traps moored at four sites between NW Africa and the Caribbean (i.e., CB-20°N/21°W, at 1214 m; M1-12°N/23°W, at 1150 m; M2-14°N/37°W, at 1235 m; M4-12°N/49°W, at 1130 m). Highest coccolith-CaCO₃ fluxes at the westernmost site M4, where the nutricline is deepest along the tropical North Atlantic, were dominated by deep-dwelling small-sized coccolith species *Florisphaera profunda* and *Gladiolithus flabellatus*. Total coccolith-CaCO₃ fluxes of 371 mg m⁻² yr⁻¹ at M4 were followed by 165 mg m⁻² yr⁻¹ at the north-easternmost CB, 130 mg m⁻² yr⁻¹ at M1, and 114 mg m⁻² yr⁻¹ at M2 in between. Coccoliths accounted for nearly half of the total carbonate flux at M4 (45%), much higher compared to 23% at M2 and 15% at M1 and CB. At site M4, highest ratios of coccolith-CaCO₃ to particulate organic carbon fluxes and weak correlations between the carbonate of deep-dwelling species and particulate organic carbon suggest that increasing productivity in the lower photic zone in response to ocean warming might enhance the *rain ratio* and reduce the coccolith-ballasting efficiency. The resulting weakened biological carbon pump could, however, be counterbalanced by increasing frequency of Saharan dust outbreaks across the tropical Atlantic, providing mineral ballast as well as nutrients to fuel fast-blooming and ballast-efficient coccolithophore species.

Introduction

Among mineralizing phytoplankton, coccolithophores (Haptophyta) are the most important group of unicellular marine algae, covering their cells with a calcified exoskeleton (the coccosphere) composed of numerous tiny, calcified scales (~ 1 to 20 μm across), the so-called coccoliths (Pienaar 1994). Coccolithophores are among the main functional

phytoplankton groups, crucial for the biologically mediated fixation and conversion of atmospheric CO₂ to organic carbon (via photosynthesis), and its subsequent export to the deep ocean, also termed “biological carbon pump” (BCP) (Cermeño et al. 2008). Coccolithophores contribute less to global marine primary production (~ 1–10%) compared to diatoms, which are the main exporters of particulate organic carbon (POC) in the modern ocean (e.g., Poulton et al. 2007; Malviya et al. 2016 and refs. therein). Yet, they are among the main exporters of particulate inorganic carbon (PIC) from the photic zone to the deep sea, thereby performing a unique dual role in the ocean’s carbon cycle since 220 million years ago, when they first appeared in the geological record (e.g., Rost and Riebesell 2004; Broecker and Clark 2009; Hutchins 2011). Following the death of the cells, some of the coccolith-CaCO₃

*Correspondence: cataguerreiro@fc.ul.pt

This is an open access article under the terms of the Creative Commons Attribution-NonCommercial-NoDerivs License, which permits use and distribution in any medium, provided the original work is properly cited, the use is non-commercial and no modifications or adaptations are made.

Additional Supporting Information may be found in the online version of this article.

may dissolve within the photic zone (Poulton et al. 2006) while most of it sinks out of the surface waters inside zooplankton fecal pellets and marine snow aggregates or incorporated into the agglutinating shells of tintinnid microzooplankton (Knappertsbusch and Brummer 1995 and refs. therein).

The ratio of biogenic PIC to POC export from the surface down to the deep ocean, termed the *rain ratio*, is a key parameter for biogeochemical models exploring the long-term efficiency of atmospheric CO₂ drawdown (Archer and Maier-Reimer 1994; Zondervan 2007). It represents the opposing relationship between the production of organic matter acting as a CO₂ sink (via photosynthesis) and the production of CaCO₃ acting as a CO₂ source (via calcification) (e.g., Rost and Riebesell 2004; Hutchins 2011 and refs. therein). As the *rain ratio* is what largely determines the biologically mediated CO₂ flux between the ocean and the overlying atmosphere (e.g., Rost and Riebesell 2004; Cermeño et al. 2008), any changes in the PIC and POC fluxes triggered by shifts in the coccolithophore communities are likely to alter the earth's climate. While nutrient depletion triggered by increasing thermal stratification is more likely to favor coccolithophores over diatoms (e.g., Rivero-Calle et al. 2015), the subsequent increase of PIC production is likely to weaken the efficiency of the BCP through increasing the *rain ratio*. This may however be counterbalanced by coccolithophores providing ballast material acting to accelerate the sinking velocities of organic-rich aggregates formed at the surface (Armstrong et al. 2002; Ziveri et al. 2007; Fischer and Karakas 2009). This is supported by up to 83% of global POC fluxes being reportedly linked to CaCO₃ (Klaas and Archer 2002), reflecting the high density of calcite, and its higher abundance in the open ocean compared to terrigenous material (e.g., Klaas and Archer 2002; Ziveri et al. 2007).

Given the unequivocal importance of coccolithophores for the ocean's carbon cycle (Rost and Riebesell 2004; Zondervan 2007; Hutchins 2011), significant attention has been given to exploring the dynamics of their export production over the last few decades, particularly in the North Atlantic (e.g., Broerse et al. 2000; Sprengel et al. 2002; Guerreiro et al. 2019). Time-series sediment traps collecting settling particles (organic and inorganic) over periods of time ranging from weeks to years are the standard approach for studying the impact of seasonal variations in coccolithophore export productivity on the functioning of BCP (e.g., Milliman 1993; Baumann et al. 2005; Salter et al. 2015). However, most of the existing studies express the contribution of coccolithophores to total carbonate export in terms of total coccolith-CaCO₃ flux without discussing its dependence on the spatiotemporal dynamics of ecologically distinct species. In addition, most observations report from mid- to high-latitude regions in the NE Atlantic Ocean, where coccolith production is more seasonal and dominated by fast-blooming placolith-bearing species (e.g., *Emiliania huxleyi*) compared to low-latitude open-ocean regions (e.g., Broerse et al. 2000; Sprengel et al. 2002;

Romero et al. 2020). As tropical oceans provide a benchmark for future primary productivity in increasingly warmer and nutrient-depleted waters, it is crucial to constrain the main drivers of coccolith-CaCO₃ export in these regions.

Here, we provide a synoptic, synchronized, and biweekly resolved record of coccolith-CaCO₃ fluxes of the more abundant species across the entire tropical North Atlantic, in relation to atmospheric and oceanographic processes. The study builds on an earlier transatlantic transect extending downwind from NW Africa (off Cape Blanc) to the Caribbean (Fig. 1; Supplementary Table S1), right underneath the core of the main dust plume originating from the Saharan desert (Guerreiro et al. 2019). Here, we relate coccolith-CaCO₃ fluxes with other biogenic particle fluxes collected at four trap sites, including total biogenic carbonate, biogenic silica and organic matter, as well as POC (e.g., Fischer et al. 2012, 2013; Korte et al. 2017). The molar ratio between the fluxes of coccolith-CaCO₃ and POC (Coccolith-CaCO₃/POC) and the species-specific coccolith-ballasting effect are analyzed to investigate how ecologically different species modulate the export of organic carbon. The spatiotemporal flux distribution of atmospheric dust along the transect (van der Does et al. 2020) is also included to explore links between Saharan dust deposition and coccolith-CaCO₃ export production. For understanding the processes involved, we combine our in situ transatlantic observations with time series of surface-water concentrations of chlorophyll *a* (Chl *a*) and PIC determined by satellite remote sensing during the same year.

Environmental settings

Our study is based on time-series material from four sediment trap moorings collecting sinking particles during ~ 1 yr along a transatlantic transect extending from the Caribbean into the mesotrophic region offshore Cape Blanc (NW Africa) (Fig. 1; Supplementary Table S1). Traps M4 (12°N 49°W), M2 (14°N 37°W), and M1 (12°N 23°W) collected particles in synchronous intervals of 16 d, from 19 October 2012 to 07 November 2013, while trap CB (21°N 20°W) collected particles at variable intervals, from 04 October 2012 to 21 February 2014. Details of the mooring equipment, the deployment/recovery of the sediment traps, and the treatment of the recovered sample bottles are described in the cruise reports by Stuu et al. (2013) and Fischer et al. (2012, 2013, 2014).

Wind-forced oceanographic processes, both geostrophic and seasonal, and transatlantic Saharan dust deposition have been recently reported to influence the distribution of coccolith species fluxes along the studied transect during the monitored sampling interval (Guerreiro et al. 2017, 2019). The region is characterized by westward deepening of the nutricline related to large-scale geostrophic deepening of the thermocline from the eastern to the western tropical North Atlantic (Merle 1980; Katz 1981). In contrast, the

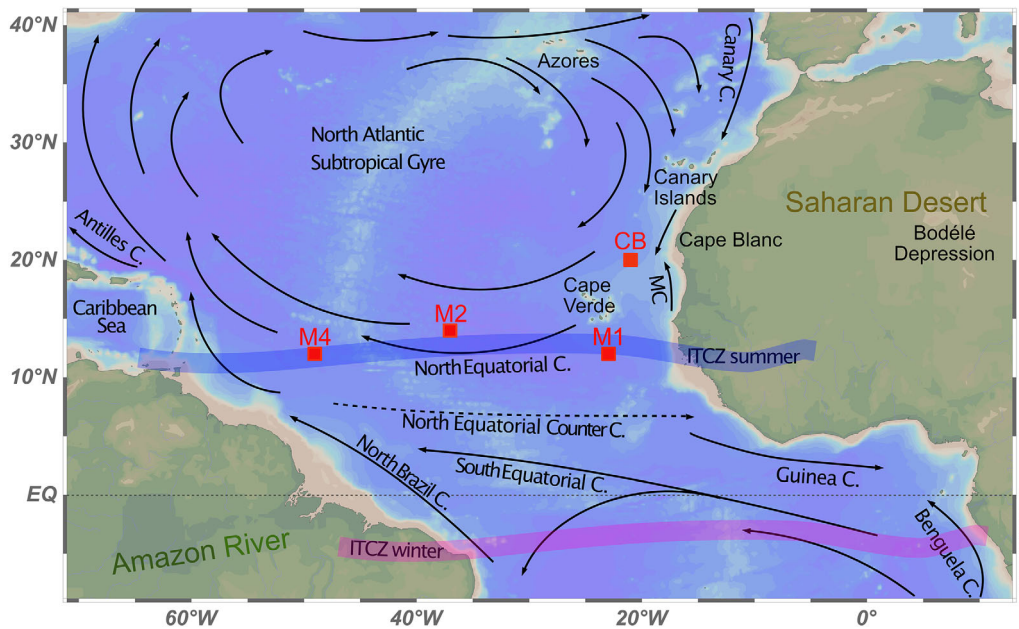


Fig 1. Location of the trap mooring sites M4, M2, M1, and CB and a schematic representation of the main surface currents in the equatorial Atlantic Ocean, including the Mauritanian Current (MC) flowing northwards off NW Africa (see Guerreiro et al. 2019 and refs. therein).

dynamics of the seasonal mixed layer depth is function of wind forcing over the uppermost $\sim 75\text{--}80$ m water depth along the transect (Guerreiro et al. 2019). Seasonality was weak and atmospheric conditions were similar at all four locations, modulated by the seasonal migrations of the Intertropical Convergence Zone (Basha et al. 2015; Guerreiro et al. 2019; see Fig. 1). Higher precipitation rates, weaker trade winds, and enhanced thermal stratification occurred in summer and autumn, while little to no precipitation, intensified winds and a deeper mixed layer depth in winter and spring. Toward the northeast, conditions were less influenced by the Intertropical Convergence Zone but mostly determined by variable magnitude of yearlong upwelling off Cape Blanc (Pastor et al. 2013 and refs. therein).

Carbonate fluxes were on average higher at M4 ($41 \text{ g m}^{-2} \text{ d}^{-1}$) and M1 ($38 \text{ g m}^{-2} \text{ d}^{-1}$) compared to the oligotrophic site M2 ($22 \text{ g m}^{-2} \text{ d}^{-1}$), while the fluxes of organic matter and biogenic silica were higher at M1, followed by M4 and M2 (Korte et al. 2017). New flux data from trap CB indicate the highest fluxes of carbonate ($92 \text{ g m}^{-2} \text{ d}^{-1}$) and organic matter along the transect, reflecting the high productivity of calcifying plankton induced by upwelling (Fischer et al. 2016; Guerreiro et al. 2019; Romero et al. 2020). While the organic matter fluxes at CB were only slightly higher compared to the eastern site M1, the fluxes of biogenic silica were lower. Saharan dust fluxes available for sites M1 (14 g m^{-2}), M2 (3 g m^{-2}), and M4 (3 g m^{-2}) were highest at M1 forced by strong trade-wind intensities at lower altitudes during spring, as well as following the occurrence of sporadic dust storms during summer/autumn (van der Does et al. 2020). Site M4 was marked by the occurrence of two high surface productivity events in

April and October–November 2013, triggered by combination of enhanced dust deposition, wind-forced mixing, and fresh-water dispersal linked to the seasonal inflow of the Amazon River Plume into the western part of the transect (e.g., Mollere et al. 2010; Guerreiro et al. 2017; Korte et al. 2020). The sediment trap samples bulk composition at all four sites is presented in Supplementary Table S4.

Methods

Laboratory and microscope analysis

For the detailed description of the procedures regarding the treatment of the sediment trap samples, the readers are referred to Fischer et al. (2016) and Korte et al. (2017). Procedures for the coccolith analysis detailed in Guerreiro et al. (2017, 2019), including the coccolith species counting method and the calculation of coccolith fluxes. The coccolith-derived CaCO_3 export fluxes were determined using the mass equation of Young and Ziveri (2000), according to which the coccolith mass of distinct coccolithophore species is expressed as:

$$\text{Coccolith calcite (pg)} = 2.7 \times k_s \times l^3$$

in which $2.7 =$ density of calcite (CaCO_3); $k_s =$ shape constant; $l =$ coccolith size (mostly distal shield length). The size of around 3500 coccoliths was measured from most species present in samples from traps M1, M2, and M4 using a Zeiss DSM 940A scanning electron microscope. Most of the used coccolith shapes come from Young and Ziveri (2000). For some of the species, the shape constants have been slightly adjusted within their shape range, as

indicated in Young and Ziveri (2000), such that a meaningful relationship would be achieved between the coccolith masses of the measured species. The measured coccolith lengths and the subsequently determined species-specific coccolith masses are provided in Supplementary Table S2. For trap CB, the coccolith-CaCO₃ masses are based on coccolith measurements performed by Köbrich and Baumann (2009) for the same location. The only exceptions to this include *Gladiolithus flabellatus*, *Hayaster perplexa*, *Oolitothus antillarum*, and *Umblicosphaera hulburtiana* for which we used the actual measurements of coccoliths from the neighboring trap site M1. Carbonate content of rare coccolith species for which we did not perform size measurements was based on coccolith size information available from Nannotax (<http://www.mikrotax.org/Nannotax3/>) and estimates from Young and Ziveri (2000) (Supplementary Table S2). A multivariate statistical analysis using Principal Components Analysis (PCA, correlation mode; PAST-3 software) and a Pearson correlation coefficient matrix were undertaken to explore and statistically support the observed relationships between species-specific coccolith-CaCO₃ fluxes and the other particle fluxes (Supplementary Information).

Satellite remote sensing

Time series of sea surface concentrations of Chl *a* and PIC were obtained from satellite remote sensing, used as proxies for phytoplankton biomass (see Guerreiro et al. 2017, 2019) and coccolithophore carbonate surface production across the transect (e.g., Balch et al. 2005) (data sets details provided in

Supplementary Table S3). The PIC product has been validated in various locations with in situ measurements (e.g., Balch et al. 2005), providing considerable insights into the phenological characteristics of coccolithophore surface blooms at a global scale (e.g., Hopkins et al. 2015). Both Chl *a* and PIC data were retrieved for each trap location using a 2° × 2° latitude-longitude area around the trap location and averaged for each sediment trapping interval. The box, corresponding to ~108 × 108 Nm (1° = ~59 Nm), was taken as representative of the catchment area of a trap deployed at 1200 m depth, given the mean sinking speed of marine phytoplankton and algal aggregates (e.g., Waniek et al. 2000). Data were processed for the study period of October 2012–October/November 2013 at sites M1, M2, and M4, and up to January 2014 at site CB.

Results and discussion

Coccolith-carbonate export production

The coccolith-CaCO₃ fluxes were highest and most seasonally variable at the opposite ends of the transatlantic array, particularly at the westernmost site M4, while lower and less seasonally variable fluxes occurred at the more central sites in between, particularly at mid ocean site M2 (Fig. 2a). From October 2012 to October–November 2013, site M4 received a total of 371 mg m⁻², followed by M1 (130 mg m⁻²) and M2 (114 mg m⁻²), while from October 2012 to January 2014, site

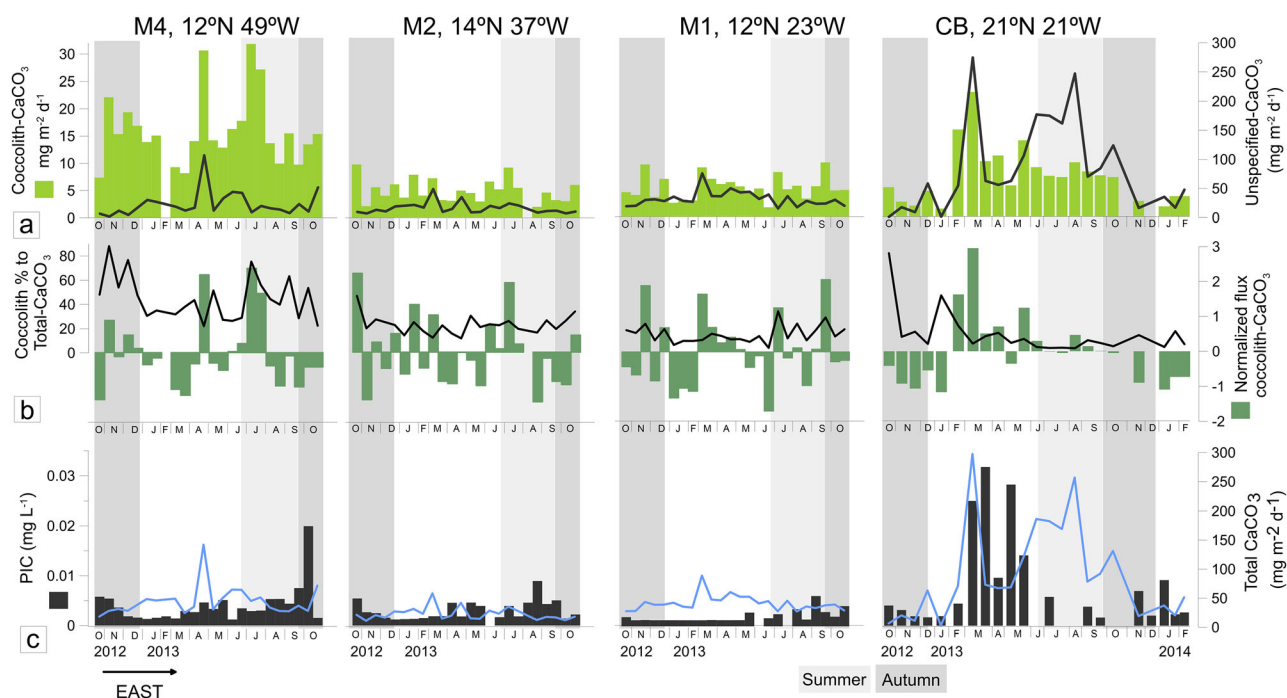


Fig 2. Fluxes of coccolith-CaCO₃ (light green bars) and unspecified-CaCO₃ (black line) (a), deviation from the annual mean coccolith-CaCO₃ flux at each trap site (dark gray bars) and percent contribution of coccoliths carbonate to total CaCO₃ flux (b), total carbonate flux (blue line) and particulate inorganic carbon (PIC) concentration at the ocean surface (c) at sites M4, M2, M1, and CB. Light and dark gray vertical bars indicate summer and autumn, respectively.

CB received a total of 165 mg m⁻². Highest fluxes at M4 and CB ultimately reflect the higher coccolith export production closer to the Caribbean and to the upwelling-induced high-productivity region off NW Africa, compared to the more open and oligotrophic sites M1 and M2 (Fig. 2a). The 2–3 times higher fluxes at M4 mirror the much higher coccolith export productivity reported by Guerreiro et al. (2019) compared to the other trap sites, including the mesotrophic and carbonate-dominated region off Cape Blanc.

Albeit occasional mismatches, the temporal distribution of carbonate produced by coccolithophores was similar to that of the total carbonate flux (Fig. 2a,c) and of the unspecified-CaCO₃ flux. The latter is assumed to include carbonate from coccolith fragments and coccoliths within aggregates (which were not included in the counts) and/or produced by other calcifying planktonic organisms (Fig. 2a). Significant differences were noticed, however, between the distribution of surface PIC and carbonate fluxes from our in situ trap records (Fig. 2c). Much higher PIC with markedly distinct seasonality at site CB compared to the other sites indicates that the satellite PIC data only represent a portion of the coccolith-CaCO₃ production between NW Africa and the Caribbean, particularly at the more open ocean sites M1–M4. Site CB was the region where surface PIC was both highest (up to 0.032 mg L⁻¹ in early spring) and more seasonally similar to coccolith- and total-carbonate fluxes, all three strikingly peaking during spring (Figs. 2c). We also observed a PIC pulse in early October 2013 at the westernmost site M4 (up to 0.02 mg L⁻¹ in M4-23), which did coincide with surface ocean fertilization (recorded by the trap at 1200 m depth in M4-24; Guerreiro et al. 2017; Korte et al. 2020), and reaching concentrations almost as high as the spring peak recorded offshore Cape Blanc (Fig. 2c). Still, the drastic drop of surface PIC south

westwards of CB (~ 0.01 mg L⁻¹ at site M1) suggests a much lower coccolith-CaCO₃ export at the other sites, which is not what we find in the traps, especially in M4 (Fig. 2c).

Such seemingly contradicting observations seem related to technical limitations related to the maximum satellite-observation depth range, reflecting the transition from a more markedly dynamic region with a shallower nutricline at CB toward a nearly permanently stratified ocean setting (see Guerreiro et al. 2019). That coccolith-CaCO₃ fluxes at site CB were mostly produced by fast-blooming surface-dwelling species including the dominant *E. huxleyi* (Fig. 3), probably contributes to produce larger and denser surface blooms that are optically reflective enough to be detected by remote sensing (e.g., Holligan et al. 1993; Balch et al. 2018). On the other hand, highest coccolith contribution to carbonate in October 2012 at site CB not reflected in terms of PIC (Fig. 2b,c) suggests that either coccolithophores were temporarily thriving below the satellite depth range or that coccolith-CaCO₃ production and export were not coupled. This illustrates the extent to which the remotely sensed PIC is strongly limited by the optical depth of the water column (Gordon and McCluney 1975) in spite of its successful application to explore the occurrence and frequency of large-scale coccolithophore surface blooms in the North Atlantic (e.g., Balch et al. 1991; Holligan et al. 1993; Shutler et al. 2013). This presents a major constraint for detecting coccoliths in tropical regions where coccolithophores typically thrive at greater depths (Poulton et al. 2017). While massive surface blooms shown by satellites may have a crucial biogeochemical impact on regional scales (Iglesias-Rodríguez et al. 2002), they probably represent a minor fraction compared to the background levels of CaCO₃ produced annually on a global scale.

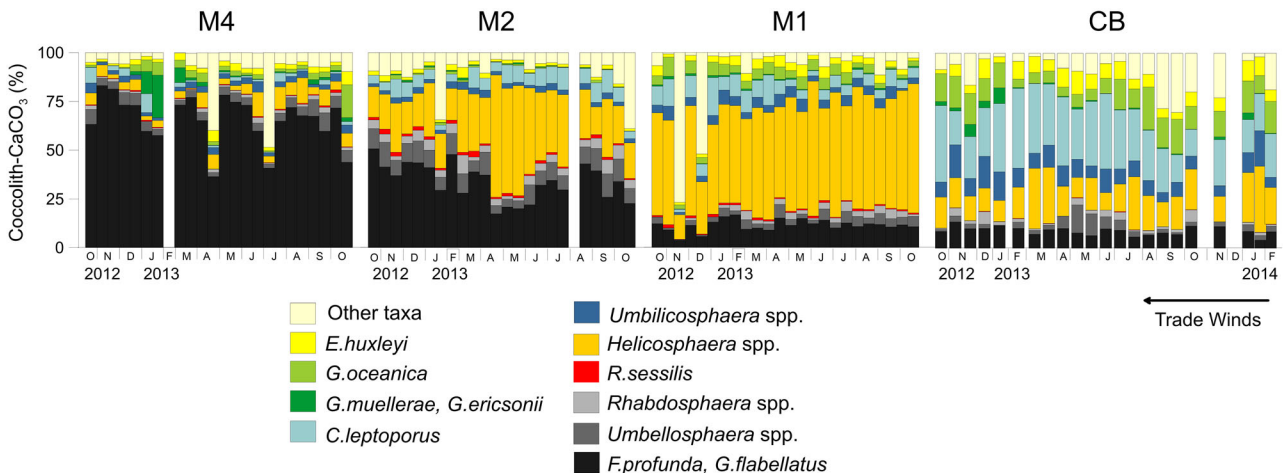


Fig 3. Percent coccolith-CaCO₃ production by the most abundant sinking coccolithophore taxa at trap sites M4, M2, M1, and CB. Taxa similar in spatio-temporal distribution were grouped together.

Species contributions

As expected, large-sized taxa such as *Helicosphaera* spp. and *Calcidiscus leptoporus* showed the highest coccolith- CaCO_3 mass, followed by *Rhabdosphaera* spp., *Umbellosphaera* spp., *Umbilicosphaera* spp., *Gladiolithus flabellatus*, *Gephyrocapsa oceanica*, *G. muelleriae*, *Florisphaera profunda*, *Emiliana huxleyi* and *G. ericsonii* (Fig. 4; Supplementary Table S3). While differences between taxa were a persistent feature at all four trap locations, certain species varied substantially in carbonate mass along the transect. For example, *C. leptoporus* showed a clear coccolith mass increase from west to east, while *G. flabellatus* revealed the opposite tendency. Taxa such as *G. oceanica*, *Rhabdosphaera* spp. and *U. foliosa* had their highest carbonate mass at site CB and their lowest at site M1, while *Helicosphaera* spp. was more heavily calcified at sites CB and M2 (Fig. 4).

The subsequently determined coccolith- CaCO_3 fluxes revealed, however, that both large-sized *Helicosphaera* spp. ($1.6 \text{ mg m}^{-2}\text{d}^{-1}$) and smaller-sized species such as *G. flabellatus* ($2.3 \text{ mg m}^{-2}\text{d}^{-1}$) and *F. profunda* ($1 \text{ mg m}^{-2}\text{d}^{-1}$) contributed the most to the mean transatlantic coccolith- CaCO_3 production, with 26%, 17%, and 13%, respectively. The latter were followed by *C. leptoporus* ($0.8 \text{ mg m}^{-2}\text{d}^{-1}$; 11%), and by *G. oceanica*, *Umbellosphaera* spp., *Umbilicosphaera* spp., and *E. huxleyi* ($0.2\text{--}0.5 \text{ mg m}^{-2}\text{d}^{-1}$; 4–5%), while the remaining taxa individually contributed less than 4%. Of these, *G. ericsonii*, *G. muelleriae*, and *Reticulofenestra sessilis* produced less than $0.1 \text{ mg m}^{-2}\text{d}^{-1}$ (Supplementary Table S4).

Species constituting less than 5% of the total coccolith sinking assemblage (Guerreiro et al. 2019) contributed a total of $1 \text{ mg m}^{-2}\text{d}^{-1}$.

In terms of seasonality, higher coccolith- CaCO_3 fluxes in spring and summer along the transect (Fig. 2b) reflect the seasonal latitudinal migration of the Intertropical Convergence Zone modulating the temporal dynamics of taxa with distinct ecological preferences (Basha et al. 2015; Guerreiro et al. 2017). Enhanced thermal stratification resulting from weaker winds across the tropical North Atlantic in summer and autumn led to increased carbonate produced by species more typical of the lower photic zone (LPZspp.) (Figs. 3 and 5c). By contrast, enhanced wind-forced mixing leading to cooler and more nutritious surface conditions in winter and spring has favored carbonate export by placolith-bearing taxa more typical of the upper photic zone (UPZspp).

Placolith-bearing taxa produced higher carbonate fluxes at both ends of the transect, with *C. leptoporus* dominating at the northeastern site CB and *gephyrocapsid* species at the western site M4. Higher carbonate production by *C. leptoporus*, *E. huxleyi*, and *Umbilicosphaera* spp. at site CB reflects their higher affinity for more seasonally variable and upwelling-influenced settings off Cape Blanc compared to the other locations (Figs. 3 and 5a, see Guerreiro et al. 2019). Similar seasonal distribution between the fluxes of coccolith- CaCO_3 by these taxa and of total CaCO_3 at CB highlights the link between the productivity of placolith-bearing taxa and carbonate production in this mesotrophic region (Fischer and

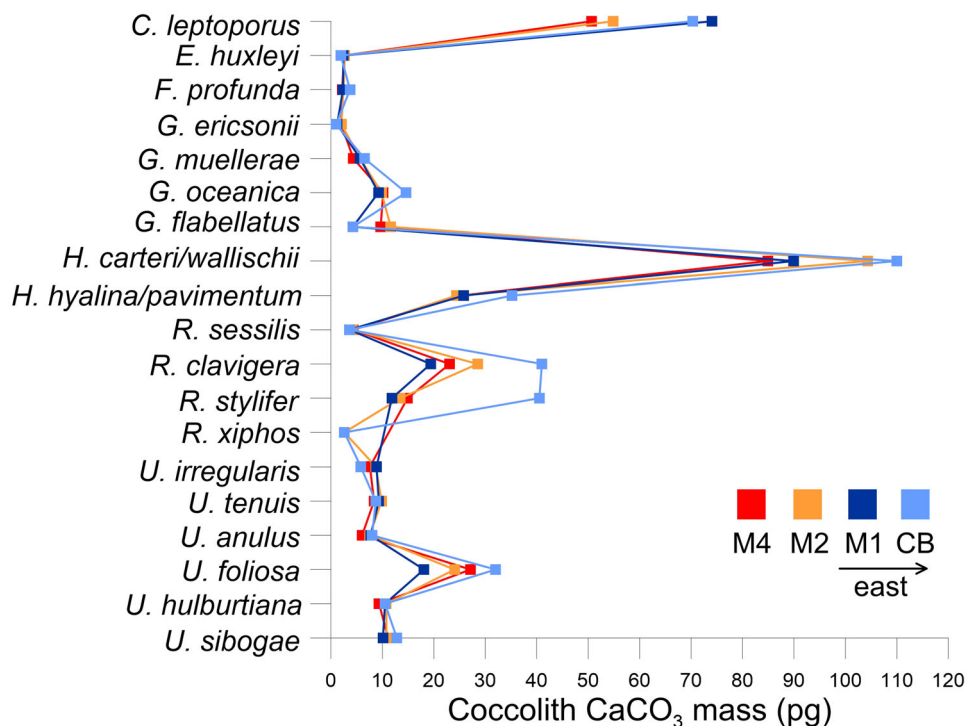


Fig 4. Mean species-specific carbonate mass (in pg) of coccoliths species from the most abundant sinking species at trap sites M4, M2, M1, and CB.

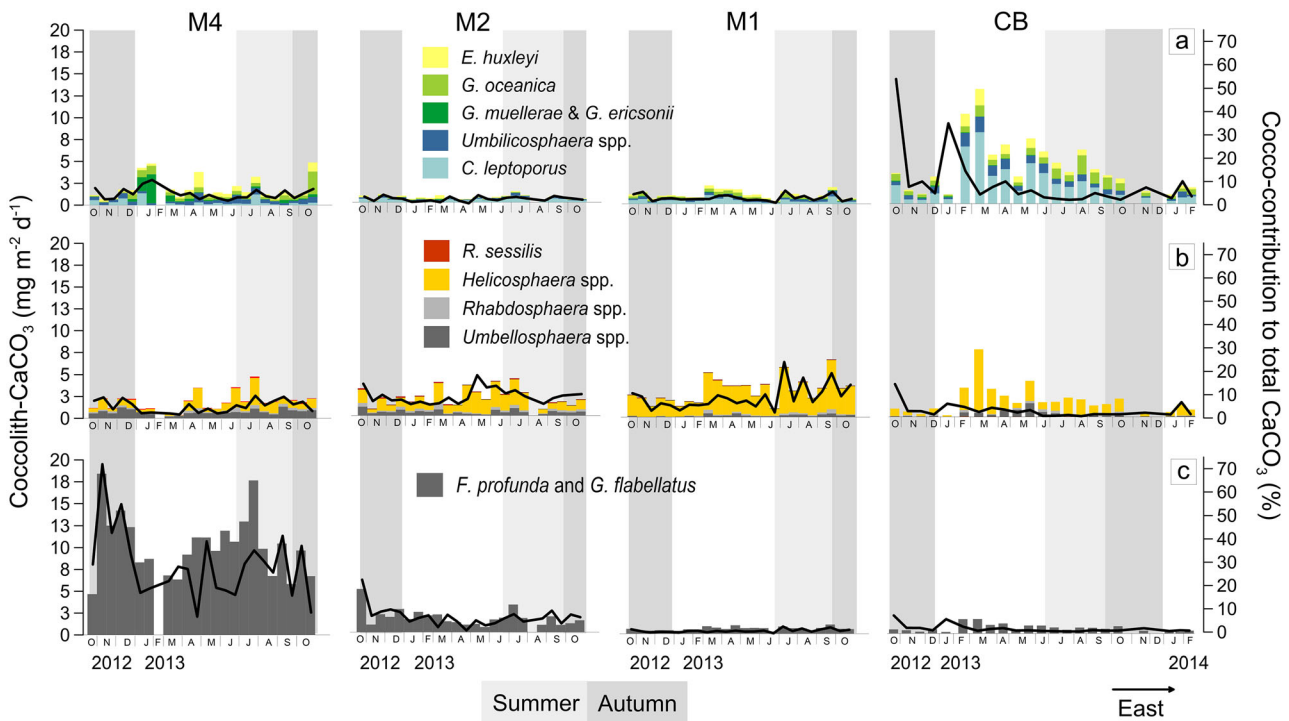


Fig 5. Fluxes of coccolith- CaCO_3 (left y-axes) and percentage of total carbonate (right y-axes) produced by the most abundant coccolithophore taxa at sites M4, M2, M1, and CB. Taxa with a similar spatiotemporal distribution (see Guerreiro et al. 2019) were grouped into: (a) placolith-bearing *E. huxleyi*, *G. oceanica*, *G. muelleriae* and *G. ericsonii*, *Umbilicosphaera* spp. and *C. leptoporus*, (b) *Helicosphaera* spp., *Rhabdosphaera* spp., *Umbellosphaera* spp., *R. sessilis*, and (c) lower photic zone species (LPZspp) *F. profunda* and *G. flabellatus*.

Karakas 2009; Romero et al. 2020). Of these species, the low-flux and large-sized *C. leptoporus* contributed the most (up to 41% of coccolith- CaCO_3 production in the winter-spring transition).

Pulsed coccolith- CaCO_3 export production by *G. muelleriae*, *G. ericsonii*, *G. oceanica*, and *E. huxleyi* in January, April, and October–November 2013 at site M4 (M4-6-7, M4-12, and M4-24, respectively) contributed to slightly increase the flux temporal variability in this area compared to M2 and M1 (Fig. 5a). Carbonate fluxes produced by these species during such high surface productivity events were similar or even higher compared to their maxima at the upwelling-influenced site CB (Fig. 5a). During the spring and autumn events, mineral dust, organic matter, and biogenic silica, as well as the UPZspp/LPZspp ratio (i.e., ratio between coccolith fluxes of the upper photic zone species *E. huxleyi* and *G. oceanica*, and the lower photic zone species *F. profunda* and *G. flabellatus*, used as a proxy for the nutricline depth dynamics; Guerreiro et al. 2017, 2019) (Figs. 6a,f), also increased. Such combination of proxies marks the occurrence of surface ocean fertilization resulting from dust deposition combined with wind-forced vertical mixing and Amazon water dispersal, all three processes seasonally influencing site M4 (Guerreiro et al. 2017; Korte et al. 2017, 2020). These ecologically r-selected events were clearly illustrated in the results from the principal

components analysis (PC1 and PC2, Supplementary Fig. S1 and Table S5), providing evidence on the potential of short-term upper photic zone productivity for enhancing coccolithophore contribution to total carbonate flux in highly stratified tropical settings.

Helicosphaera spp. were by far the dominant coccolith- CaCO_3 producers at the more central sites, particularly at M1, but also reaching high fluxes at site CB. That these species produced more carbonate during both spring and summer suggest a strong affinity for well-illuminated conditions in the photic zone but a lesser dependency on stratification and nutrient availability/supply (Figs. 3 and 5b). *Rhabdosphaera* spp. and *Umbellosphaera* spp. produced higher carbonate fluxes at sites M4 and M2, showing a rather weak seasonality along the entire transect. Carbonate by *Rhabdosphaera* spp. was slightly higher at M2 and M1 compared to *Umbellosphaera* spp., which were more productive at M4 throughout the year, and during spring at CB. *R. sessilis* revealed low coccolith- CaCO_3 along the entire transect but slightly higher at site M2 (Figs. 3 and 5b).

Higher species-specific coccolith-carbonate production along the transect by *Helicosphaera* spp. and *C. leptoporus* (Fig. 4) supports previous notions that total coccolith-carbonate flux is largely determined by larger species in spite of their lower productivity (e.g., Broerse et al. 2000; Young

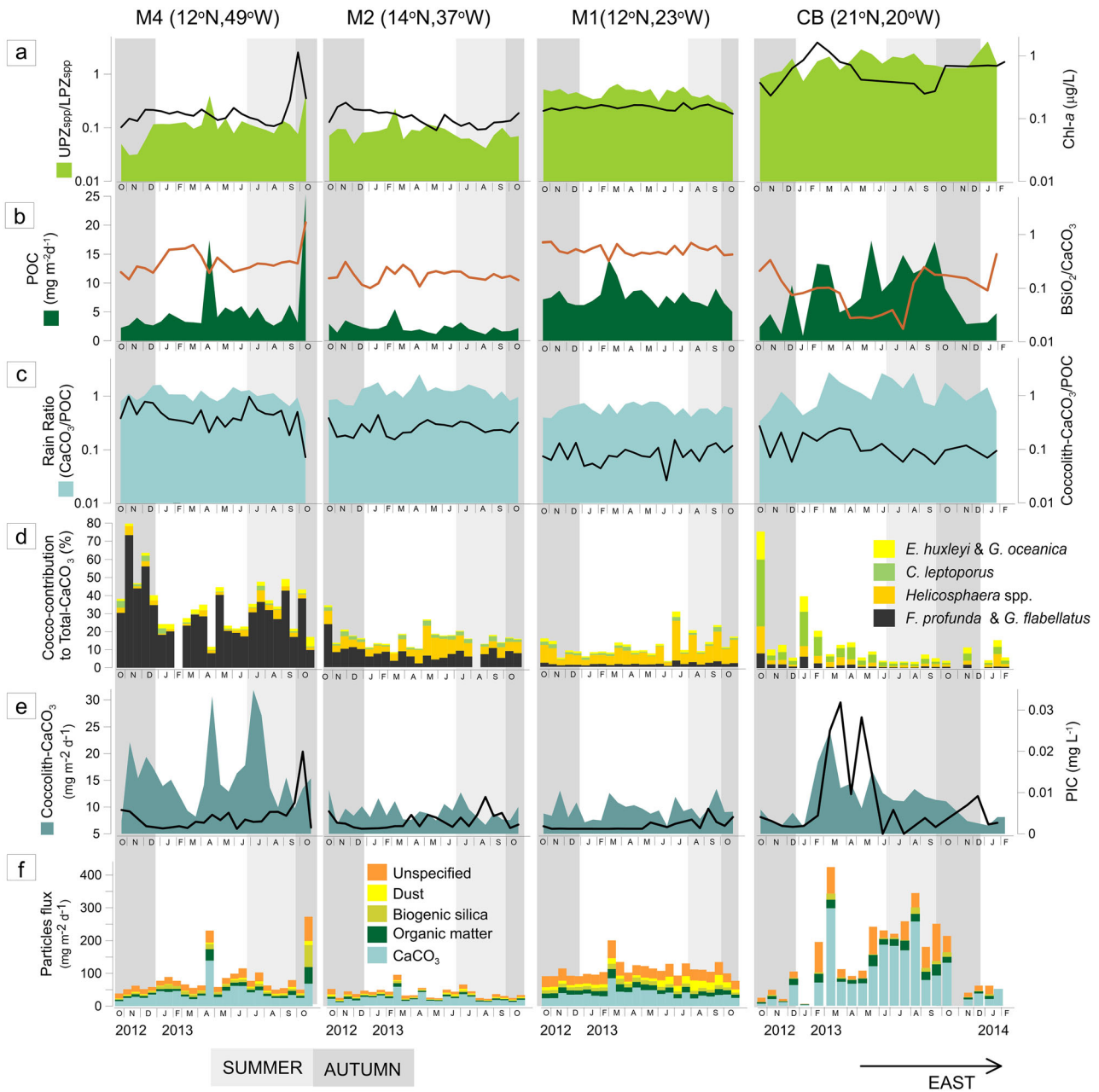


Fig 6. Spatiotemporal variation of (a) UPZspp/LPZspp ratio (light green) in coccolith fluxes of *E. huxleyi* and *G. oceanica* typical of the upper photic zone (UPZ), and *F. profunda* and *G. flabellatus* typical of the lower photic zone (LPZ) (used as a proxy for nutricline depth dynamics; Guerreiro et al. 2017, 2019), and surface chlorophyll *a* concentrations (Chl *a*, black line); (b) total fluxes of particulate organic carbon (POC) (green) and molar ratio between fluxes of biogenic silica (bSiO₂) and total CaCO₃ (bSiO₂/CaCO₃, orange line) as a proxy for the ratio of silicifying to calcifying plankton (see Cermeño et al. 2008), (c) rain ratio (CaCO₃/POC, in blue) and Coccolith-CaCO₃/POC molar ratios (black line); (d) relative contribution of coccolith-CaCO₃ to total CaCO₃ fluxes by the most important carbonate producing coccolith taxa; (e) total coccolith-CaCO₃ fluxes (blue) and surface ocean concentrations of particulate inorganic carbon (PIC) (black line); and (f) fluxes of (from bottom to the top) CaCO₃, organic matter, biogenic silica, and lithogenic dust (M1, M2, and M4 data from Korte et al. 2017 and van der Does et al. 2020). The mass flux of unspecified particles (i.e., residual fraction) results from subtracting the weights of biogenic constituents (i.e., CaCO₃, organic matter and biogenic silica) from the total mass and has been used as a proxy for dust deposition in the Atlantic Ocean (Jickells et al., 1998), including our study area (e.g., Fischer et al. 2016; Guerreiro et al. 2017; Korte et al. 2017).

and Ziveri 2000; Baumann et al. 2004). This is also the case for the rare but very large-sized species *Scyphosphaera apsteinii*, included in the category “others,” which produced up to

15 mg m⁻²d⁻¹ at site M4 (Supplementary Table S3). Still, and albeit their much lighter and smaller-sized coccoliths, *G. flabellatus* and *F. profunda* were the most important

carbonate producers along the transect, contributing to 2–3 times higher coccolith- CaCO_3 flux at M4 ($16 \text{ mg m}^{-2} \text{ d}^{-1}$) compared to the other sites ($8 \text{ mg m}^{-2} \text{ d}^{-1}$ at CB and $5 \text{ mg m}^{-2} \text{ d}^{-1}$ at M1 and M2) (Figs. 3 and 5c). Higher mean fluxes by LPZspp at M4 ($10 \text{ mg m}^{-2} \text{ d}^{-1}$ representing 66%), even compared to large-sized *Helicosphaera* spp. at site M1 (52%) and *C. leptopus* at site CB (27%) (Supplementary Table S4), highlight the importance of coccolith- CaCO_3 production in the lower photic zone in highly stratified settings typical of tropical oceans (Guerreiro et al. 2019).

The observed spatiotemporal patterns in species-specific carbonate fluxes were also reflected in terms of their relative contributions to total carbonate flux. Maximum coccolith percent contribution of 82% in the autumn-winter 2012–2013 at site CB was dominated by *C. leptopus* (up to 32%) (Fig. 5a), to which *Helicosphaera* spp. (up to 13%) (Fig. 5b) and *G. oceanica* (12%) (Fig. 5a) also contributed. At site M4, highest carbonate contributions were during the autumn 2012 and summer 2013, dominated by *F. profunda* and *G. flabellatus* (up to 37%) (Fig. 5c), whereas *Helicosphaera* spp. contributed the most throughout the year at sites M2 and M1 (up to 22%) (Fig. 5b).

Coccolithophores and carbonate export

Both the total- and coccolith-carbonate export fluxes across the transect were generally in line with previous trap studies in the North Atlantic. While carbonate fluxes at sites M4, M2, and M1 (15 , 8 , and $14 \text{ g m}^{-2} \text{ yr}^{-1}$, respectively) were much higher compared to $2\text{--}5 \text{ g m}^{-2} \text{ yr}^{-1}$ reported as typical of central ocean gyres, site CB ($34 \text{ g m}^{-2} \text{ yr}^{-1}$) falls within the $30\text{--}40 \text{ g m}^{-2} \text{ yr}^{-1}$ described as characteristic of eastern boundary upwelling systems (Milliman 1993) (Supplementary Table S4). Likewise, coccolith- CaCO_3 fluxes of $1.8 \text{ g m}^{-2} \text{ yr}^{-1}$ at M2 and M1 were slightly higher compared to previous studies from the western tropical North Atlantic ($13^\circ\text{N}/54^\circ\text{W}$) (Steinmetz 1991) and near the Canary Islands (ESTOC- $29^\circ\text{N}/17^\circ\text{W}$ and LP- $29^\circ\text{N}/17^\circ\text{W}$; Sprengel et al. 2002). At site M4, however, mean fluxes of $5.8 \text{ g m}^{-2} \text{ yr}^{-1}$ were higher not only compared to M1, M2, and CB and to the sites mentioned above, but also to other locations at higher latitudes in the North Atlantic. These include the Sargasso Sea (Honjo 1978), the Bay of Biscay (MS1- $44.5^\circ\text{N}/2.5^\circ\text{W}$; Beaufort and Heussner 1999), and the temperate and subtropical North Atlantic (NABE48- $48^\circ\text{N}/21^\circ\text{W}$ and NABE34- $34^\circ\text{N}/21^\circ\text{W}$; Broerse et al. 2000; Ziveri et al. 2000). In contrast, mean fluxes of $2.9 \text{ g m}^{-2} \text{ yr}^{-1}$ offshore Cape Blanc were nearly half of the $4.9 \text{ g m}^{-2} \text{ yr}^{-1}$ earlier reported for the same site (Köbrich and Baumann 2009), pointing to substantial interannual variability in this mesotrophic region.

Albeit the similar or even higher export of coccolith- CaCO_3 observed across the tropical North Atlantic compared to more seasonal regimes at higher latitudes, the average coccolith contribution to the total carbonate was only 45% at M4, 23% at M2, and 15% at M1 and CB (see Figs. 2b and 6d). These

values show a clear westward increasing contribution of coccolithophores to total carbonate production along the tropical North Atlantic. While the percent contribution at the most oligotrophic site M2 is in line with some of the locations above, site M4 was substantially higher, also compared to, for example, the 39% and 24% in the subtropical and temperate eastern North Atlantic, respectively (Broerse et al. 2000), and to 28–33% off the Canary Islands (Sprengel et al. 2002). Köbrich and Baumann (2009) report a contribution of 18% in 1988–1989 at site CB that is similar to M1 and CB during our studied period, but lower than at M4 and M2. The only regions in the North Atlantic reporting even lower percentages include the Bay of Biscay (12%; Beaufort and Heussner 1999) and the western tropical North Atlantic (9% at $13^\circ\text{N}/54^\circ\text{W}$; Steinmetz 1991). Although total mass fluxes along the tropical North Atlantic are all dominated by biogenic carbonate (Fig. 6f; Supplementary Table S4), M4 was the only location approaching the conventional notion of coccolithophores dominating carbonate production and export in the global ocean (e.g., Baumann et al. 2004; Baumann and Freitag 2004; Broecker and Clark 2009).

Similar fluxes of coccolith- and total-carbonate at sites M2, M1 and CB compared to previous trap studies suggest that coccolith dissolution did not cause the observed low percentages, consistent with the notion that coccolith preservation in North Atlantic sediments is excellent (lysocline at $\sim 4000\text{--}4500 \text{ m}$; Milliman 1993; Milliman et al. 1999 and refs. therein). A certain proportion of broken coccoliths that were not included in the coccolith- CaCO_3 budget could, however, contribute to underestimate the coccolithophorid percent contributions. This is supported by previous traps studies reporting that such coccolith fragments add to the coccolith-dominated sediment size fraction (Knappertsbusch and Brummer 1995; Ziveri et al. 2007). Such biogenic remnants, which also include other carbonate particles of both biogenic (including juvenile foraminifera) and non-biogenic origin, appear to significantly add to the so-called biogenic carbonate powder (Ziveri et al. 2007).

Biological breakage and partial dissolution of coccoliths by zooplankton grazing, as well as driven by microbial oxidation of organic matter in flocculates and aggregates, could also explain the much lower coccolith percent contributions at the eastern sites CB and M1 (Knappertsbusch and Brummer 1995; Milliman et al. 1999 and refs. therein). Higher surface Chl *a* concentrations, as well as higher UPZspp./LPZspp. ratios and POC fluxes off Cape Blanc (Fig. 6a,b), rooted in strong and yearlong coastal upwelling (Pastor et al. 2013), could result in higher carbonate removal rates compared to the highly stratified open ocean regions at M4 and M2 (Milliman et al. 1999). This is in line with reportedly observed differences in species diversity between plankton and sediment traps samples linked to the selective destruction of smaller and/or more delicate forms during sinking (e.g., holococcolithophores) (Baumann et al. 2005 and refs. therein). Some authors go even further to

suggest that only the coccoliths and coccospheres that sink incorporated intact inside of fecal pellets and marine snow aggregates, or into the shells of tintinnid microzooplankton, are likely to be preserved in the traps (Knappertsbusch and Brummer 1995; Beaufort and Heussner 1999; Baumann et al. 2005 and refs. therein). Thereby, export productivity is also a function of daily fluctuations in the production of larger biogenic particles (Knappertsbusch and Brummer 1995; Fischer et al. 2009) and of the factors modulating their own seasonal ecological dynamics. Whereas these processes may have led to underestimate the sinking coccoliths from which the coccolith-CaCO₃ fluxes were calculated, enhanced proportions of the “biogenic carbonate powder” would still contribute to the observed total carbonate fluxes. This is supported by the general agreement between the coccolith- and unspecified-CaCO₃ fluxes, which may include a significant coccolith contribution (Fig. 2a).

Other calcifying planktonic organisms (e.g., foraminifera, pteropods, heteropods, calcareous dinophytes) could have also contributed more carbonate than it is usually assumed. As most studies dealing with these issues do not include foraminifera < 150 μm, which make up a large but poorly constrained fraction of the total foraminifera, their total relative contribution to the carbonate flux is likely to be underestimated (Brummer et al. 1986). This is supported by occasional pulsed coccolith-CaCO₃ fluxes coinciding with decreased coccolith percent contributions to carbonate flux along the transect, suggesting that other calcifying organisms were playing a greater role for carbonate production (e.g., April and October–November 2013 at M4, early March 2013 at M1, and February–March 2013 at CB) (Figs. 2b and 5a).

Finally, the volumetric/biometric method used in our study (Young and Ziveri 2000) could have also contributed to underestimating the species-specific coccolith-CaCO₃ fluxes, since it is only applicable for intact coccoliths and assuming an identical shape and width proportions for all individual coccoliths of the same species (Ziveri et al. 2007). While some of these issues have been reportedly reduced with methods based on the coccoliths’ optical properties (i.e., calcite birefringence used for estimating the coccolith-carbonate mass; Beaufort 2005; Beaufort et al. 2014; Bollmann 2014, Fuertes et al. 2014), the latter are not exempt of uncertainties. In fact, important errors have been reported, driven by difficulties in calibrating the microscope light intensity for measuring coccolith calcite, with subsequent uncertainties on the coccolith mass estimates. Secondly, the optical method is not applicable to weakly birefringent coccoliths nor to coccoliths thicker than a certain valid measurable thickness. This results in the systematic weight underestimation in coccolith calcite from larger taxa compared to the morphometric method, and the exclusion of the larger coccoliths that are often the most important coccolith-carbonate contributors (Beaufort et al. 2014; Bollmann 2014; Fuertes et al. 2014; Rigual

Hernández et al. 2020) (see Table 2). Therefore, the volumetric/biometric method was assumed to be the most advantageous for our transatlantic data set, since both the taxonomic analysis and the morphometric measurements of the coccoliths had been performed using a scanning electron microscope (Guerreiro et al. 2017, 2019). This is undoubtedly the most accurate approach for identifying coccoliths to the species level, as well as for measuring the coccoliths length, allowing to produce a consistent coccolith biogeochemical data set without the errors linked to the optical/birefringence analysis. It also provided for accurately measuring the coccoliths’ length of all species, independently of their thickness and birefringence.

Overall, our study suggests that existing notions on the relative contribution by distinct calcifying plankton groups to total carbonate export may not be accurately constrained, albeit the potentially underestimated coccolith-CaCO₃ contributions presented here. Quantifying the coccolith-CaCO₃ inside fecal pellets and marine snow aggregates (see Knappertsbusch and Brummer 1995; Beaufort and Heussner 1999) and within the “biogenic carbonate powder” (Ziveri et al. 2007) is likely to increase the accuracy of estimated coccolithophore contribution to total carbonate flux.

Coccolithophore carbonate and the rain ratio

In spite of the much higher POC fluxes at sites M1 and CB (Fig. 6b), as expected from its higher proximity to a productive eastern boundary upwelling system (e.g., Chavez et al. 2011; Signorini et al. 2015), the *rain ratio* remained fairly stable along the entire transect, only slightly lower at site M1 (Fig. 6c). This highlights the importance of biogenic carbonate production toward the eastern tropical North Atlantic. The Coccolith-CaCO₃/POC ratios, however, clearly decreased from west to east, reaching 2–4 times higher mean ratios at sites M4 and M2 (Fig. 6c), in line with the westward increase of the coccolith percent contribution to total carbonate flux discussed above. This clearly suggests an increasing role of coccolithophores in modulating the *rain ratio* toward more stratified conditions, compared to other calcifying organisms.

Higher Coccolith-CaCO₃/POC ratios at M4 were mostly produced by lower photic zone species *F. profunda* and *G. flabellatus* (see Figs. 6d and 7b). The negative correlation between the Coccolith-CaCO₃/POC and the UPZspp/LPZspp-CaCO₃ ratios (Fig. 8b) shows just that, while also illustrating the increasing role of coccolithophores in rising the *rain ratio* with the deepening of the nutricline toward the west. This is consistent with the alkalinity model of Sarmiento et al. (2002) yielding higher *rain ratios* in the tropics possibly linked to a dominant contribution by low-latitude non-bloom forming coccolithophores to global calcification. In addition, discrepancies in the size and carbonate mass of *G. flabellatus* along the transect, with twice heavier coccoliths at M4 and M2, seem to have substantially contributed to increase the total coccolith-CaCO₃ fluxes and Coccolith-CaCO₃/POC ratios

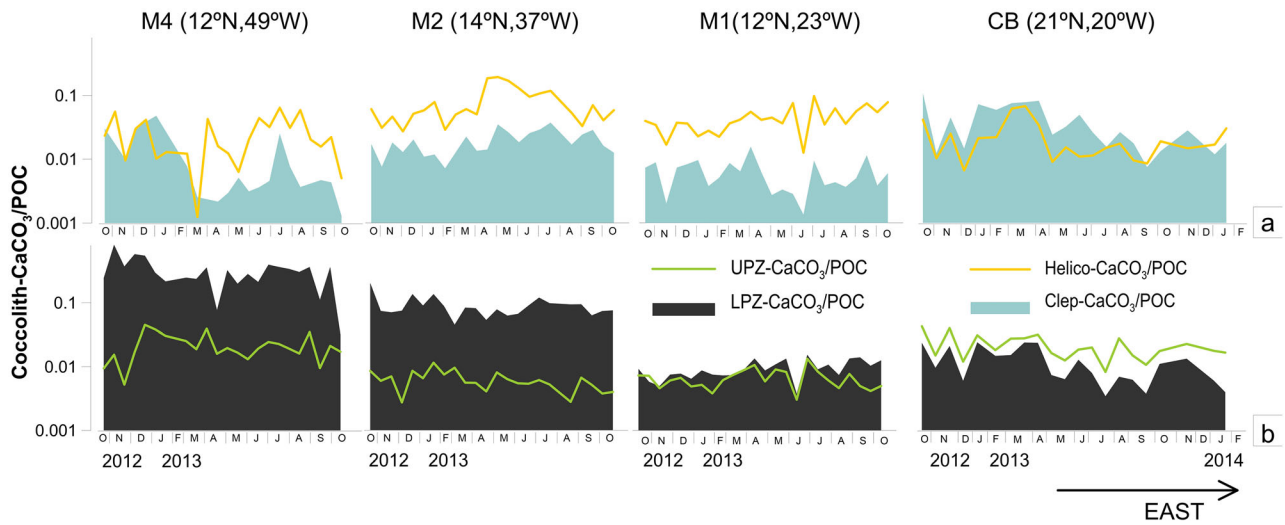


Fig 7. Spatiotemporal variation in the molar ratios of Coccolith- CaCO_3 to particulate organic carbon (POC) fluxes produced by (a) *Helicosphaera* spp. (yellow line) and *C. leptoporus* (brakish green) and (b) LPZ species *F. profunda* and *G. flabellatus* (black) and the UPZ species *E. huxleyi* and *G. oceanica* (green line) (where UPZ and LPZ stand for upper- and lower-photic zones).

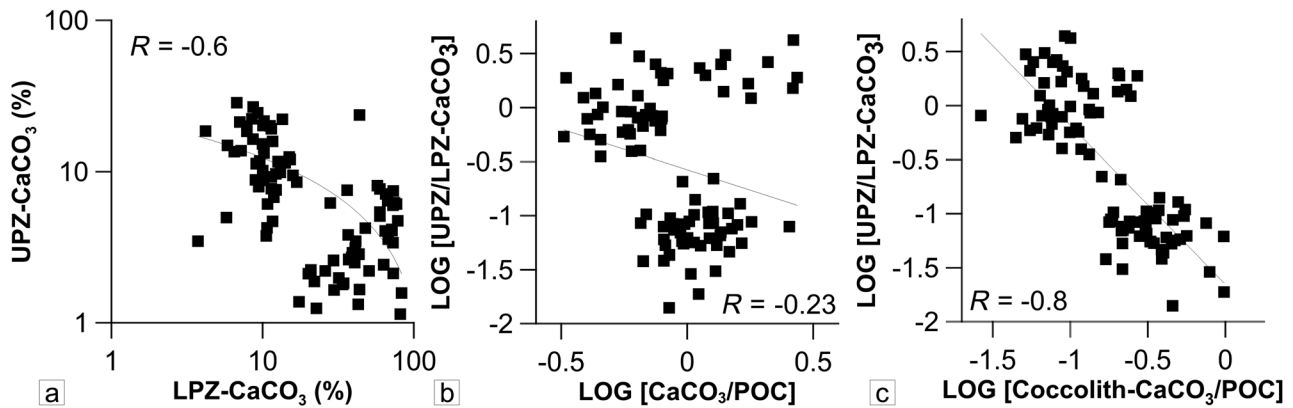


Fig 8. Relationships between (a) percentages of UPZ spp.- CaCO_3 and LPZ spp.- CaCO_3 , and between the UPZ spp./LPZ spp.- CaCO_3 ratio (where UPZ spp. and LPZ spp. stand for species typical of the upper- and lower-photic zones) and (b) the *rain ratio*, that is, ratio of CaCO_3 to particulate organic carbon (POC) fluxes, and (c) the Coccolith- CaCO_3 to POC molar ratios, along the transatlantic transect.

toward the west. Whether this is linked to differently sized morphotypes of *G. flabellatus* and/or to a greater susceptibility of its calcification to increasingly dynamic water conditions toward NW Africa remains as an open question.

Assuming that deep-dwelling species are ecologically better adapted to thrive in the face of ocean warming (Guerreiro et al. 2019), our 1-yr transatlantic snapshot suggests that coccolithophore communities are likely to become less calcified in response to ocean stratification. This is in line with Beaufort et al. (2011) who projected a decline in coccolith mass through ecological selection of less-calcified species rather than from reduced calcification within individual species. In other words, the biogeochemical impact of coccolithophores may be mostly due to variations in abiotic factors affecting their ecology (i.e., temperature, stratification/

mixing, light and nutrient availability), to which some taxa are more resilient than others (e.g., Poulton et al. 2007; Zondervan 2007; Sett et al. 2014). But while a decline in coccolithophore calcification would be expected to reduce the *rain ratio* (e.g., Beaufort et al. 2011; Hutchins 2011), our observations indicate just the opposite. Indeed, yearlong-dominant lower photic zone species produced 3–8 times higher Coccolith- CaCO_3 /POC ratios at M4 even compared to ratios by much larger-sized *Helicosphaera* spp. and *C. leptoporus* at M1 and CB (see Fig. 7a,b).

Lower Coccolith- CaCO_3 /POC ratios at M1 compared to M2 reflect the yearlong higher POC fluxes toward east (Fig. 6b,c). Although site M1 is marked by low coccolithophore export production, high fluxes of POC and biogenic silica in this region (Fig. 6f) suggest an increase in productivity linked to a

dominant surface-dwelling phytoplankton assemblage (including diatoms) in response to the eastward shallowing of the nutricline (Romero and Fischer 2017; Guerreiro et al. 2019). This is supported by the rising $bSiO_2/CaCO_3$ ratios from M4 to M1 (Fig. 6b), in parallel with surface Chl *a* concentrations and the UPZspp/LPZspp ratio (Fig. 6a). Lower and more seasonally variable $bSiO_2/CaCO_3$ ratios just at the mesotrophic site CB (Fig. 6c), however, suggest a much higher production of calcifying plankton compared to silicifying plankton. While eastern boundary upwelling systems are more traditionally linked to diatom production (Abrantes et al. 2016), the observed high POC fluxes offshore Cape Blanc are associated to carbonate-dominated production instead. Pteropod-dominated carbonate production reported by Fischer et al. (2016) may explain the observed high *rain ratios*, low Coccolith- $CaCO_3$ /POC ratios, and low coccolith contribution to total $CaCO_3$ flux observed at the mesotrophic site CB.

Assuming that higher *rain ratios* result in a slower BCP, the similar *rain ratios* observed at both the upwelling-site CB and the thermally stratified sites M4 and M2 suggest that the BCP was not more efficient off NW Africa, contrary to expectations from a region close to such a productive eastern boundary upwelling system (see Fischer et al. 2009, 2016, 2019). Our transatlantic observations further suggest that increased coccolithophore productivity in the lower photic zone in response to ocean warming is unlikely to lower the *rain ratio*. On the contrary, if combined with a decreased biological drawdown of atmospheric CO_2 due to nutrient depletion, the relative increase of these species may actually contribute to weaken the BCP (see Cermeño et al. 2008). This argues for a potentially greater role of export productivity from the lower photic zone in marine carbon cycling in the face of ocean warming.

Coccolith-ballasting

The incorporation of mineral ballast—such as biogenic carbonate—in marine snow aggregates and fecal pellets adds to their density, thereby increasing their sinking velocities. This is critical for reducing the exposure of POC to remineralization during settling, hence ensuring its successful downward export and sequestration in the deep ocean (Armstrong et al. 2002; Fischer et al. 2016, 2019; van der Jagt et al. 2018). Positive correlation between POC and carbonate produced by coccoliths (Fig. 9a), as well as by other calcifying plankton groups (i.e., unspecified- $CaCO_3$ flux, Fig. 9b) along the transect, does suggest such a link between carbonate ballasting and POC sequestration (Supplementary Table S7). This is consistent with previous observations based on regional (Fischer et al. 2009; Fischer and Karakas 2009) and global-scale sediment trap records (Ziveri et al. 2000, 2007; Klaas and Archer 2002), as well as from model simulations (Armstrong et al. 2002).

Strongest correlations between coccolith- $CaCO_3$ and POC export were found at sites M2 and CB, while the unspecified-

$CaCO_3$ flux was more consistently linked to POC at all sites (Fig. 9a,b). At M4, the correlation strongly depends on two outliers representing distinct events of Amazon and possibly dust fertilization of the upper photic zone in the western tropical North Atlantic (i.e., Guerreiro et al. 2017; Korte et al. 2017, 2020). The importance of these outliers at M4 is also reflected in the stronger correlation between upper photic zone species and POC export toward the western part of the transect (Fig. 9d), consistent with the pulsed carbonate production by *E. huxleyi* and *G. oceanica* in spring and autumn. Overall, the positive correlation between the UPZspp/LPZspp- $CaCO_3$ ratio and POC fluxes (Fig. 9d—all sites; Supplementary Table S7) reflects the enhanced coccolith- $CaCO_3$ production in the upper photic zone linked to higher productivity in shallower nutricline conditions, whether due to geostrophic wind forcing (i.e., sites CB and M1) or to the occurrence of transient surface blooms (site M4; see Guerreiro et al. 2017, 2019; Korte et al. 2020).

In spite of the much higher unspecified- $CaCO_3$ fluxes compared to coccolith- $CaCO_3$ (Fig. 2a), the ratio between coccolith- and unspecified- $CaCO_3$ shows little correlation to the POC export at individual trap sites (Fig. 9c), and only a weak negative correlation over the entire transect (Fig. 9c—all sites, Supplementary Table S7). This suggests a minor coccolith-ballasting effect relative to other calcifying groups, and that compositional changes in the calcifying plankton community might, to some degree, alter the efficiency of POC export along the transect.

More efficient coccolith-ballasting has been reported from the NE Atlantic, where coccolith- $CaCO_3$ fluxes are dominated by *C. leptoporus* (Ziveri et al. 2007). This species was also the main coccolith-carbonate producer in the northeast of our transect (Fig. 5a) and was positively correlated to POC fluxes at site CB (Supplementary Table S6 and Fig. S2). However, higher carbonate contributions by other taxa toward the southwest, including both large- and small-sized coccolith species, resulted in weaker correlations with POC, for example, large-sized *Helicosphaera* spp. compared to smaller-sized *E. huxleyi* and *G. oceanica* (Supplementary Table S6 and Fig. S2). The efficiency of coccolith-ballasting seems, hence, to be less related to the coccolith-carbonate mass but more with the species' affinity to bloom in high productivity conditions, which, in turn, are linked to higher POC fluxes. Supporting this hypothesis is the lack of correlation between POC and the lower photic zone species *F. profunda* and *G. flabellatus*, not only at sites M4 and M2 where they dominate coccolith- $CaCO_3$ production, but also elsewhere along the transect (see Supplementary Table S6 and Fig. S2). Lower POC production/export from the lower photic zone in highly stratified conditions could explain the reduced ballasting efficiency of these deep-dwelling species, in spite of their high carbonate contribution.

Our data suggest that coccoliths will be more effective ballasts when produced by fast-blooming surface-dwelling species

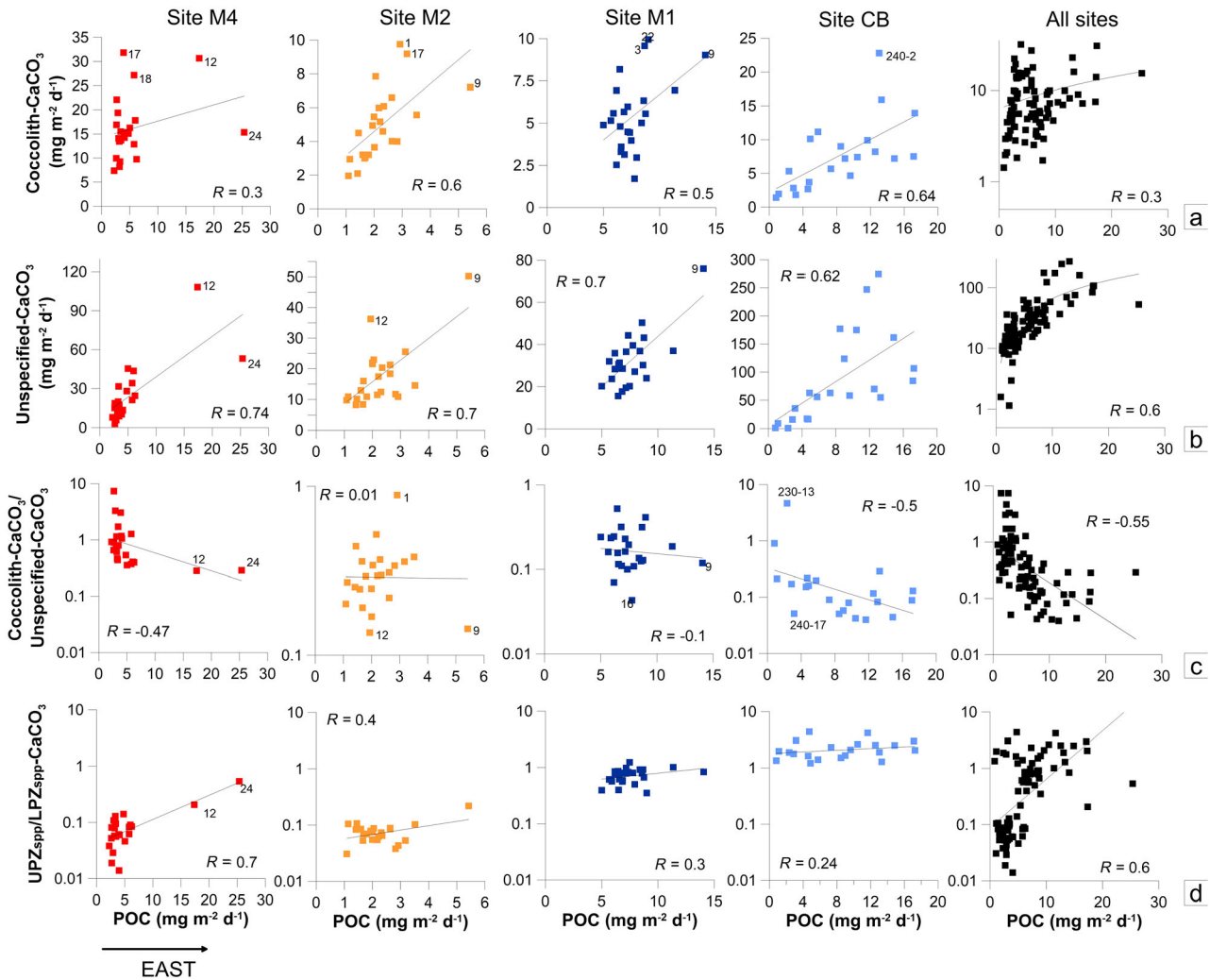


Fig 9. Correlation between particulate organic carbon (POC) fluxes and (a) total coccolith- CaCO_3 fluxes, (b) unspecified- CaCO_3 fluxes, (c) the ratio between coccolith- and unspecified- CaCO_3 fluxes, and (d) ratio between the coccolith- CaCO_3 fluxes produced by taxa typical of the upper- and lower-photic zone ($\text{UPZ}_{\text{spp}}/\text{LPZ}_{\text{spp}}\text{-CaCO}_3$). POC flux data for M1, M2, and M4 from Korte et al. (2017). See Corresponding Pearson correlation matrix in Supplementary Table S7.

such as *E. huxleyi* and *G. oceanica*. Not only these species have higher affinity to thrive in more productive conditions, they are also more likely to be grazed upon by microzooplankton compared to larger taxa like *Helicosphaera* spp. and *C. leptopus* (Rost and Riebesell 2004), thus increasing their chances to sink inside fecal pellets. It seems that the production/export of organic matter is what modulates the efficiency of coccolith-ballasting, in line with Passow and De La Rocha (2006) and Fischer et al. (2016) who argued that the POC flux determines the flux of minerals to the deep ocean and not vice-versa.

Coccolithophore carbonate and Saharan dust

Being adjacent to the world's largest source of soil dust, our transatlantic region is a natural laboratory to explore the effects of Saharan dust deposition in the marine environment,

not only as a source of mineral ballast but also as a nutrient fertilizer to fuel coccolithophore productivity. Indeed, as referred above, our data do show a sharp increase in carbonate of *G. oceanica* and *E. huxleyi* (Fig. 5a) during the Amazon and possibly dust fertilization of the upper photic zone in the western tropical North Atlantic, reflecting their fast response to short-term nutrient input (i.e., Guerreiro et al. 2017; Korte et al. 2017, 2020). Interestingly, though, such coccolith-carbonate increase resulted in lower Coccolith- CaCO_3 /POC ratios due to the drastic co-increase of POC during these dusty events (Figs. 6a,b). Albeit their slightly heavier coccolith mass, Coccolith- CaCO_3 /POC ratios by *E. huxleyi* and *G. oceanica* were lower even compared to those produced by deep-dwelling species at site M4 (Fig. 7b). Bory et al. (2001) also reported a drastic increase in POC fluxes following an event of high export of coccoliths by *E. huxleyi* (> 93%) and

of lithogenic particles off NW Africa, to which enhanced input of dust-born nutrients could have contributed.

Concerning the dust ballasting effect, our data do show a stronger positive correlation of POC to Saharan dust fluxes (Fig. 10a) than to coccolith- CaCO_3 (Fig. 9a), suggesting more efficient ballasting. This is consistent with the weak negative correlation between the Coccolith- CaCO_3 /dust ratio and POC along the transect (Fig. 10c—M1, M2, and M4; Supplementary Tables S7 and S8). Since there were no changes in coccolith species that would indicate dust fertilization east of M4, one might expect that increased dust ballasting with increasing proximity to the dust sources in Africa would have greatly contributed to the observed high POC export at M1 (see Supplementary Table S5 and PC2 in Fig. S1). However, the weaker correlation between POC and dust (Fig. 10a) compared to POC and coccolith- CaCO_3 fluxes at sites M2 and M1 (Fig. 9a) suggests a higher efficiency of coccolith-ballasting. It seems that dust had no clear added

effect on either POC production (via fertilization) at site M1, consistent with its negative correlation to UPZspp/LPZspp- CaCO_3 (Fig. 10b), nor in promoting its export (via ballasting) in this region.

For the mesotrophic CB, the residual (unspecified) mass flux—often used as a proxy for Saharan dust fluxes (Fischer and Karakas 2009; Fischer et al. 2016; van der Does et al. 2020)—suggests much lower dust deposition northwards of the Saharan dust plume core where M1 is located ($\sim 12^\circ \text{N}$) (Fig. 7f; Supplementary Table S4 and Fig. S3). Previous studies have reported the interaction of very high fluxes of this residual fraction with abundant formation of organic-rich marine snow particles at site CB to increase carbon sequestration offshore NW Africa relative to other eastern boundary upwelling systems (e.g., Fischer and Karakas 2009; van der Jagt et al. 2018). Although we do not have dust data for site CB to confirm in which of these eastern locations Saharan dust acted as a more

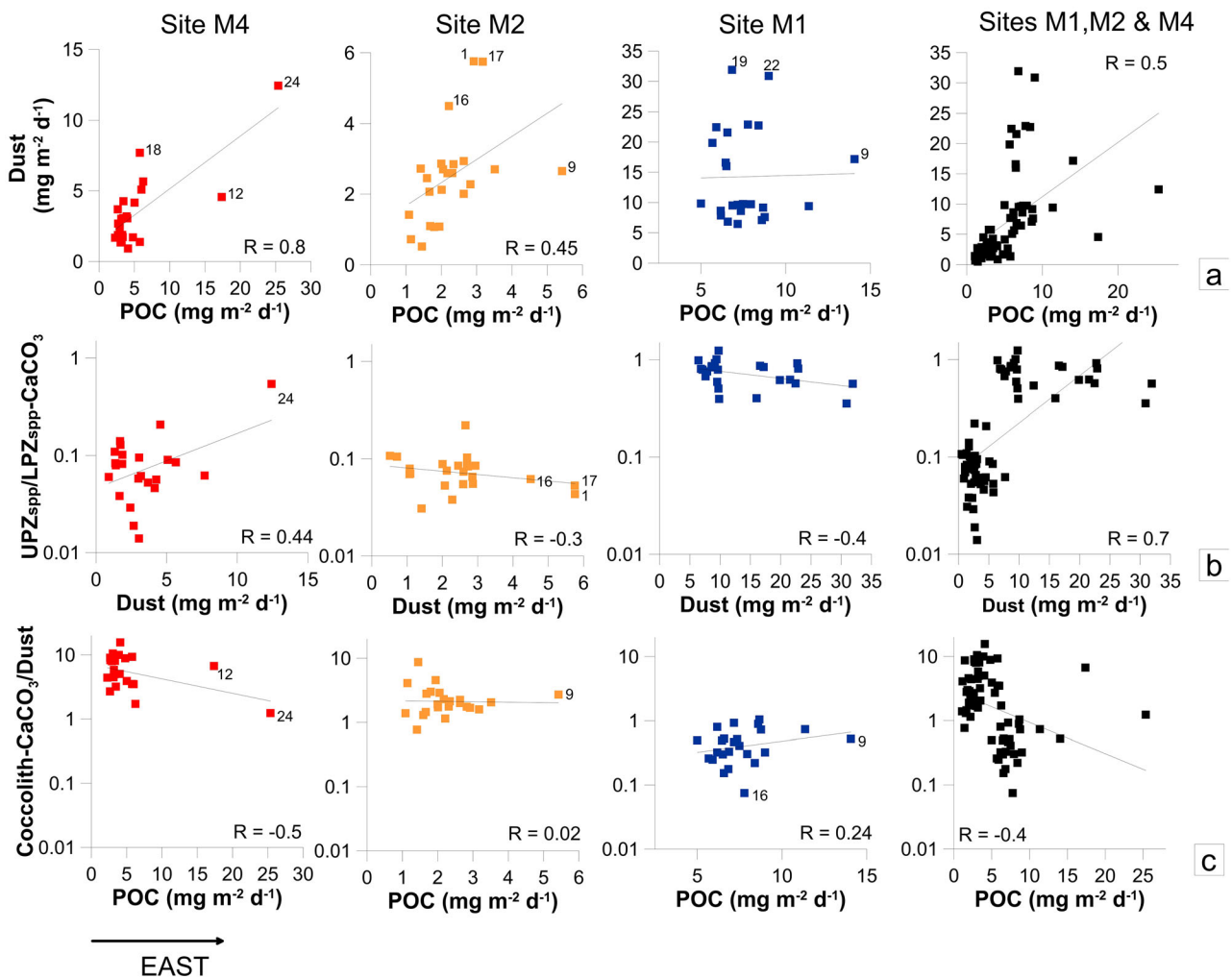


Fig 10. Correlation between (a) fluxes of dust and particulate organic carbon (POC), (b) UPZspp/LPZspp- CaCO_3 ratio (where UPZspp and LPZspp stand for species typical of the upper- and lower-photoc zones) and dust, and (c) ratio coccolith- CaCO_3 /dust and POC fluxes. POC and dust data for M1, M2, and M4 from Korte et al. (2017) and van der Does et al. (2020). See Corresponding Pearson correlation matrix in Supplementary Table S8.

effective ballast, the observed similarly weak correlation between the residual fraction and POC at both M1 and CB do not point toward any significant dust-ballasting effect in any of these locations (Supplementary Fig. S3). The proposed link between Saharan dust deposition and coccolith-CaCO₃ production in the upper photic zone is, however, reinforced by the stronger correlation between the UPZspp/LPZspp-CaCO₃ ratio and dust (Fig. 10b) compared to the residual mass flux along M1-M4 (Supplementary Fig. S3b).

Our study suggests that an increasing dominance of lower photic zone species in response to ocean warming may potentially lead to reducing the drawdown of atmospheric CO₂ by simultaneously (1) increasing the *rain ratio* and (2) reducing the coccolith-ballasting efficiency, both processes likely to weaken the BCP. Climate-driven increasing levels of atmospheric dust across the tropical North Atlantic could, however, contribute to counterbalance this tendency. Either through fertilizing the ocean and/or by acting as ballast material, dust has the potential to reduce the Coccolith-CaCO₃/POC molar ratios and to promote a more efficient coccolith-ballasting, both contributing to the accelerate the BCP.

Conclusions

Our synoptic observations of seasonally resolved coccolith-CaCO₃ export fluxes along a transatlantic transect of four sediment trap sites contribute to understand the role of calcifying phytoplankton in the total carbonate export production. The potential of coccolithophore species for influencing the BCP through modulating the *rain ratio* and ballasting POC along the tropical North Atlantic was investigated. The main conclusions are as follows:

- Fluxes of coccolith-CaCO₃ at sites M2, M1, and CB were similar or higher compared to previous trap studies at higher latitudes in the North Atlantic. At site M4, however, lower photic zone species *F. profunda* and *G. flabellatus* produced dramatically higher coccolith-CaCO₃ fluxes, contributing to 2–3 times higher coccolith-CaCO₃ production in the western tropical North Atlantic (16 mg m⁻² d⁻¹) compared to the other trap sites (5 mg m⁻² d⁻¹ at M2 and M1, and 8 mg m⁻² d⁻¹ at CB). This highlights the importance of carbonate produced by coccolithophores in stratified-oligotrophic conditions, typical of tropical oceans;
- Coccolith percent contributions of 45% to total carbonate in the western tropical North Atlantic were high compared to only 23% at M2, and 15% at M1 and CB, suggesting that other calcifying plankton were more important carbonate contributors eastwards of site M4. This points to the need for more accurately estimating the flux of distinct carbonate-producing pelagic organisms, as well as of quantifying the coccoliths within aggregates/fecal pellets and investigating the nature of particles within the “biogenic carbonate powder”;

- Remotely sensed surface PIC revealed a good potential for exploring the occurrence of coccolithophore blooms in conditions and/or regions where the nutricline is shallower, that is, toward the eastern boundary upwelling system off NW Africa and during the occurrence of transient fertilization events in open ocean stratified conditions. It is, however, unsuitable for regions and/or conditions where coccolith production occurs deeper in the photic zone, hence below the maximum satellite-observation depth range;
- Positive correlations between large-sized *Helicosphaera* spp. and POC fluxes were weaker compared to smaller-sized *G. oceanica* and *E. huxleyi*, suggesting that the efficiency of coccolith-ballasting is ecologically dependent. That is, it has less to do with the carbonate mass per species but with its affinity for thriving in more productive conditions. It is the POC flux that seems to determine the flux of coccoliths to the deep ocean and not vice versa;
- Higher Coccolith-CaCO₃/POC molar ratios and weaker correlations between the carbonate of lower photic zone species and POC fluxes at site M4 suggest that increasing abundances of *F. profunda* and *G. flabellatus* in response to ocean warming might contribute to weaken the BCP through (1) rising the *rain ratio* and (2) reducing the coccolith-ballasting efficiency.
- A striking flux increase of coccolith-CaCO₃ by fast-blooming *G. oceanica* and *E. huxleyi*, POC, and biogenic silica during two dust-related fertilization events at site M4 resulted in lower Coccolith-CaCO₃/POC molar ratios and higher bSiO₂/CaCO₃ ratios. This suggests that increasing Saharan dust outbreaks across the tropical North Atlantic will contribute to compensate the projected weakening of the BCP, either by providing nutrients to fuel fast-blooming surface-dwelling coccolithophore production and by promoting the export of POC via both dust- and coccolith-ballasting.

Our transatlantic observations suggest that changes in coccolithophore species composition and distribution in response to ocean warming are likely to result in community-level shifts in total organic and inorganic carbon production/export/ballasting by this group. This is expected to impact the cycling and sequestration of carbon at both regional and global scales. We highlight the need of addressing the role of coccolithophore ecological dynamics and species-specific carbonate production in modulating the *rain ratio* for more accurately project the functioning of the BCP in the face of ongoing climate change.

References

- Abrantes, F., P. Cermenó, C. Lopes, O. Romero, L. Matos, J. Van Iperen, M. Rufino, and V. Magalhães. 2016. Diatoms Si uptake capacity drives carbon export in coastal upwelling

- systems. *Biogeosciences* **13**: 4099–4109. doi:[10.5194/bg-13-4099-2016](https://doi.org/10.5194/bg-13-4099-2016)
- Archer, D., and E. Maier-Reimer. 1994. Effect of deep-sea sedimentary calcite preservation on atmospheric CO₂ concentration. *Nature* **367**: 260–263.
- Armstrong, R. A., C. Lee, J. I. Hedges, S. Honjo, and S. G. Wakeham. 2002. A new, mechanistic model of organic carbon fluxes in the ocean based on the quantitative association of POC with ballast minerals. *Deep-Sea Res. Pt. II* **49**: 219–236.
- Balch, W. M., P. M. Holligan, S. G. Ackleson, and K. J. Voss. 1991. Biological and optical properties of mesoscale coccolithophore blooms in the Gulf of Maine. *Limnol. Oceanogr.* **36**: 629–643.
- Balch, W. M., H. R. Gordon, B. C. Bowler, D. T. Drapeau, and E. S. Booth. 2005. Calcium carbonate budgets in the surface global ocean based on MODIS data. *J. Geophys. Res. Oceans* **110** (C7): C07001 [doi:10.1029/2004JC002560](https://doi.org/10.1029/2004JC002560).
- Balch, W. M., B. C. Bowler, D. T. Drapeau, L. C. Lubelczyk, and E. Lyczkowski. 2018. Vertical distributions of coccolithophores, PIC, POC, biogenic silica, and chlorophyll *a* throughout the global ocean. *Global Biogeochem. Cycles* **32**: 2–17 <https://doi.org/10.1002/2016GB005614>.
- Basha, G., P. Kishore, M. Venkat Ratnam, T. B. M. J. Ouarda, I. Velicogna, and T. Sutterley. 2015. Vertical and latitudinal variation of the intertropical convergence zone derived using GPS radio occultation measurements. *Remote Sens. Environ.* **163**: 262–269.
- Baumann, K.-H., and T. Freitag. 2004. Pleistocene fluctuations in the Benguela current system as revealed by coccolith assemblages. *Mar. Micropaleontol.* **52**: 195–215.
- Baumann, K.-H., B. Bockel, and M. Frenz. 2004. Coccolith contribution to South Atlantic carbonate sedimentation, p. 367–402. *In* H. R. Thierstein and J. R. Young [eds.], *Coccolithophores – From molecular processes to global impact*. Springer-Verlag.
- Baumann, K.-H., H. Andruleit, B. Bockel, M. Geisen, and H. Kinkel. 2005. The significance of extant coccolithophores as indicators of ocean water masses, surface water temperature, and paleoproductivity: A review. *Paläontol. Z.* **79**: 93–112.
- Beaufort, L., and S. Heussner. 1999. Coccolithophorids on the continental slope of the Bay of Biscay – Production, transport and contribution to mass fluxes. *Deep-Sea Res. Pt. II* **46**: 2147–2174.
- Beaufort, L. 2005. Weight estimates of coccoliths using the optical properties (birefringence) of calcite. *Micropaleontology* **51**: 1–9.
- Beaufort, L., and others. 2011. Sensitivity of coccolithophores to carbonate chemistry and ocean acidification. *Nature* **476**: 80–83. doi:[10.1038/nature10295](https://doi.org/10.1038/nature10295)
- Beaufort, L., N. Barbarin, and Y. Gally. 2014. Optical measurements to determine the thickness of calcite crystals and the mass of thin carbonate particles such as coccoliths. *Nat. Protoc.* **9**: 633–642.
- Bollmann, J. 2014. Technical note: Weight approximation of coccoliths using a circular polarizer and interference colour derived retardation estimates – (the CPR method). *Biogeosciences* **11**: 1899–1910.
- Bory, A., and others. 2001. Particle flux within different productivity regimes off the Mauritanian upwelling zone (EU-MELI program). *Deep-Sea Res. Pt. I* **48**: 2251–2282.
- Broecker, W., and E. Clark. 2009. Ratio of coccolith CaCO₃ to foraminifera CaCO₃ in late Holocene deep-sea sediments. *Paleoceanography* **24**: PA3205. doi:[10.1029/2009PA001731](https://doi.org/10.1029/2009PA001731)
- Broerse, A. T. C., P. Ziveri, J. E. van Hinte, and S. Honjo. 2000. Coccolithophore export production, species composition and coccolith-CaCO₃ fluxes in the NE Atlantic (34°N 21°W and 48°N 21°W). *Deep-Sea Res. Pt. II* **47**: 1877–1906.
- Brummer, G.-J., C. Hemleben, and M. Spindler. 1986. Planktonic foraminiferal ontogeny and new perspectives for micropaleontology. *Nature* **319**: 50–52.
- Cermeño, P., S. Dutkiewicz, R. P. Harris, M. Follows, O. Schofield, and P. G. Falkowski. 2008. The role of nutricline depth in regulating the ocean carbon cycle. *Proc. Natl. Acad. Sci. USA* **105**: 20344–20349.
- Chavez, F. P., M. Messié, and J. T. Pennington. 2011. Marine primary production in relation to climate variability and change. *Ann. Rev. Mar. Sci.* **3**: 227–260.
- Fischer, G., and G. Karakas. 2009. Sinking rates and ballast composition of particles in the Atlantic Ocean: Implications for the organic carbon fluxes to the deep ocean. *Biogeosciences* **6**: 85–102. doi:<https://doi.org/10.5194/bg-6-85-2009>
- Fischer, G., C. Reuter, G. Karakas, N. Nowald, and G. Wefer. 2009. Offshore advection of particles within the Cape Blanc filament, Mauritania: Results from observational and modelling studies. *Prog. Oceanogr.* **83**: 322–330.
- Fischer, G., Basse, A., Baumann, K.-H., Klann, M., Klawonn, I., Küchler, R., Nowald, N., and Ruhland, G. 2012. Report and preliminary results of RV POSEIDON Cruise P425. Las Palmas – Las Palmas, 16.01.2012–30.01.2012. Berichte, Fachbereich Geowissenschaften, Universität Bremen, No. 287: 32 pp.
- Fischer, G., and others. 2013. Report and preliminary results of R/V POSEIDON cruise POS445. Las Palmas – Las Palmas, 19.01.2013–01.02.2013. Berichte, MARUM – Zentrum für Marine Umweltwissenschaften, Fachbereich Geowissenschaften, Universität Bremen, No. 298: 30 pp., ISSN 2195-9633.
- Fischer, G., and others. 2014. Report and preliminary results of R/V POSEIDON cruise POS464, Las Palmas (Canary Islands) – Las Palmas (Canary Islands), 03.02. 2014–18.02.2014. Berichte, MARUM – Zentrum für Marine Umweltwissenschaften, Fachbereich Geowissenschaften, Universität Bremen, No. 304: 29 pp., ISSN 2195-7894.

- Fischer, G., and others. 2016. Deep ocean mass fluxes in the coastal upwelling off Mauritania from 1988 to 2012: Variability on seasonal to decadal time-scales. *Biogeosciences* **13**: 3071–3090. doi:<https://doi.org/10.5194/bg-13-3071-2016>
- Fischer, G., and others. 2019. Changes in the dust-influenced biological carbon pump in the canary current system: Implications from a coastal and an offshore sediment trap record off Cape Blanc, Mauritania. *Global Biogeochem. Cycles* **33**: 29 <https://doi.org/10.1029/2019GB006194>.
- Fuertes, M.-Á., J.-A. Flores, and F. J. Sierro. 2014. The use of circularly polarized light for biometry, identification and estimation of mass of coccoliths. *Mar. Micropaleontol.* **113**: 44–55. doi:<https://doi.org/10.1016/j.marmicro.2014.08.007>
- Gordon, H., and W. McCluney. 1975. Estimation of the depth of sunlight penetration in the sea for remote sensing. *Appl. Optics* **14**: 413–416.
- Gordon, H. R., G. C. Boynton, W. M. Balch, S. B. Groom, D. S. Harbour, and T. J. Smyth. 2001. Retrieval of coccolithophore calcite concentration from SeaWiFS imagery. *Geophys. Res. Lett.* **28**: 1587–1590. <https://doi.org/10.1029/2000gl012025>
- Guerreiro, C. V., K.-H. Baumann, G.-J. A. Brummer, G. Fischer, L. F. Korte, U. S. C. Merkel, H. de Stigter, and J.-B. W. Stuut. 2017. Coccolithophore fluxes in the open tropical North Atlantic: Influence of thermocline depth, Amazon water, and Saharan dust. *Biogeosciences* **14**: 4577–4599. doi:<https://doi.org/10.5194/bg-14-4577-2017>
- Guerreiro, C. V., K.-H. Baumann, G.-J. A. Brummer, G. Fischer, L. F. Korte, C. Sá, and J.-B. W. Stuut. 2019. Wind-forced transatlantic gradients in coccolithophore species fluxes. *Prog. Oceanogr.* **176**: 102140. doi:<https://doi.org/10.1016/j.pocean.2019.102140>
- Holligan, P. M., and others. 1993. A biogeochemical study of the coccolithophore, *Emiliania huxleyi*, in the north Atlantic. *Global Biogeochem. Cycles* **7**: 879–900.
- Honjo, S. 1978. Sedimentation of materials in the Sargasso Sea at a 5367 m deep station. *J. Mar. Res.* **36**: 469–492.
- Hopkins, J., S. A. Henson, S. C. Painter, T. Tyrrell, and A. J. Poulton. 2015. Phenological characteristics of global coccolithophore blooms. *Global Biogeochem. Cycles* **29**: 239–253.
- Hutchins, D. 2011. Forecasting the rain ratio. *Nature* **476**: 41–42.
- Iglesias-Rodríguez, M. D., C. W. Brown, S. C. Doney, J. Kleypas, D. Kolber, Z. Kolber, P. K. Hayes, and P. G. Falkowski. 2002. Representing key phytoplankton functional groups in ocean carbon cycle models: Coccolithophorids. *Global Biogeochem. Cycles* **16**: 1–20. doi:[10.1029/2001GB001454](https://doi.org/10.1029/2001GB001454)
- Jickells, T. D., S. Dorling, W. G. Deuser, T. M. Church, R. Arimoto, and M. Prospero. 1998. Air-borne dust fluxes to a deep water sediment trap in the Sargasso Sea. *Global Biogeochemical Cycles* **12**: 311–320.
- Katz, E. J. 1981. Dynamic topography of the sea surface in the equatorial Atlantic. *J. Mar. Res.* **39**: 53–63.
- Klaas, C., and D. Archer. 2002. Association of sinking organic matter with various types of mineral ballast in the deep sea: Implications for the rain ratio. *Global Biogeochem. Cycles* **16**: 1116. doi:[10.1029/2001GB001765](https://doi.org/10.1029/2001GB001765)
- Knappertsbusch, M., and G.-J. A. Brummer. 1995. A sediment trap investigation of sinking coccolithophores in the North Atlantic. *Deep-Sea Res. Pt. I* **42**: 1083–1109.
- Köbrich, M. I., and K.-H. Baumann. 2009. Coccolithophore flux in a sediment trap off Cape Blanc (NW Africa). *J. Nanoplankton Res.* **30**: 83–96.
- Korte, L. F., and others. 2017. Downward particle fluxes of biogenic matter and Saharan dust across the equatorial North Atlantic. *Atmos. Chem. Phys.* **17**: 6023–6040 doi:[10.5194/acp-17-6023-2017](https://doi.org/10.5194/acp-17-6023-2017).
- Korte, L. F., G.-J. Brummer, M. van der Does, C. V. Guerreiro, F. Mienis, C. I. Munday, L. Ponsoni, and S. Schouten. 2020. Multiple drivers of production and particle export in the western tropical North Atlantic. *Limnol. Oceanogr.* **9999**: 1–17. doi:[10.1002/lno.11442](https://doi.org/10.1002/lno.11442)
- Malviya, S., and others. 2016. Insights into global diatom distribution and diversity in the world's ocean. *Proc. Natl. Acad. Sci. USA* **113**: E1516–E1525, doi:[www.pnas.org/cgi/10.1073/pnas.1509523113](https://doi.org/10.1073/pnas.1509523113).
- Merle, J. 1980. Seasonal variation of heat storage in the tropical Atlantic Ocean. *Oceanol. Acta* **3**: 455–463.
- Milliman, J. D. 1993. Production and accumulation of calcium carbonate in the ocean: Budget of a non-steady state. *Global Biogeochem. Cycles* **7**: 927–957.
- Milliman, J. D., P. J. Troy, W. M. Balch, A. K. Adams, Y. H. Li, and F. T. Mackenzie. 1999. Biologically mediated dissolution of calcium carbonate above the chemical lysocline? *Deep-Sea Res. Pt I Oceanogr. Res* **46**: 1653–1669.
- Moller, G. S. F., E. M. L. Novo, and M. Kampel. 2010. Space-time variability of the Amazon River plume based on satellite ocean color. *Cont. Shelf Res.* **30**: 342–352.
- Passow, U., and C. De La Rocha. 2006. Accumulation of mineral ballast on organic aggregates. *Global Biogeochem. Cycles* **20**: GB1013. doi:[10.1029/2005GB002579](https://doi.org/10.1029/2005GB002579)
- Pastor, M. V., J. B. Palter, J. L. Pelegrí, and J. P. Dunne. 2013. Physical drivers of interannual chlorophyll variability in the eastern subtropical North Atlantic. *J. Geophys. Res. Oceans* **118**: 3871–3886.
- Pienaar, R. N. 1994. Ultrastructure and calcification of coccolithophores, p. 63–82. *In* A. Winter and W. G. Siesser [eds.], *Coccolithophores*. Cambridge University Press.
- Poulton, A. J., R. Sanders, P. M. Holligan, T. Adey, M. Stinchcombe, L. Brown, and K. Chamberlain. 2006. Phytoplankton mineralisation in the tropical and subtropical Atlantic Ocean. *Glob. Biogeochem. Cycles* **20**: GB4002 doi:[10.1029/2006GB002712](https://doi.org/10.1029/2006GB002712).
- Poulton, A. J., T. R. Adey, W. M. Balch, and P. M. Holligan. 2007. Relating coccolithophore calcification rates to

- phytoplankton community dynamics: Regional differences and implications for carbon export. *Deep-Sea Res. Pt. II Chapman Calcification Conference - Special* **54**: 538–557.
- Poulton, A. J., P. M. Holligan, A. Charalampopoulou, and T. R. Adey. 2017. Coccolithophore ecology in the tropical and subtropical Atlantic Ocean: New perspectives from the Atlantic Meridional Transect (AMT) programme. *Prog. Oceanogr* **158**: 150–170. <https://doi.org/10.1016/j.pocean.2017.01.003>.
- Rigual Hernández, A. S., and others. 2020. Coccolithophore biodiversity controls carbonate export in the Southern Ocean. *Biogeosciences* **17**: 245–263.
- Rivero-Calle, S., A. Gnanadesikan, C. E. Del Castillo, W. M. Balch, and S. D. Guikema. 2015. Multidecadal increase in North Atlantic coccolithophores and the potential role of rising CO₂. *Science* **350**: 1533–1537.
- Romero, O., and G. Fischer. 2017. Shift in the species composition of the diatom community in the eutrophic Mauritanian coastal upwelling: Results from a multi-year sediment trap experiment from 2003 to 2010. *Prog. Oceanogr.* **159**: 31–44. doi:<https://doi.org/10.1016/j.pocean.2017.09.010>
- Romero, O., K.-H. Baumann, K. Zonneveld, B. Donner, J. Hefter, B. Hamady, V. Pospelova, and G. Fischer. 2020. Flux variability of phyto- and zooplankton communities in the Mauritanian coastal upwelling between 2003 and 2008. *Biogeosciences* **17**: 187–214.
- Rost, B., and U. Riebesell. 2004. Coccolithophores and the biological pump: Responses to environmental changes, p. 99–125. *In* H. R. Thierstein and J. R. Young [eds.], *Coccolithophores: From molecular processes to global impact*. Springer.
- Salter, I., Schiebel, R., Ziveri, P., Movellan, A., Lampitt, R. S., and Wolff, G. A. 2015. Carbonate counter pump stimulated by natural iron fertilization in the Southern Ocean, 2015 Aquatic Sciences Meeting, Granada, Spain, 22–27 February 2015.
- Sarmiento, J. L., J. Dunne, A. Gnanadesikan, R. M. Key, K. Matsumoto, and R. Slater. 2002. A new estimate of the CaCO₃ to organic carbon export ratio. *Glob. Biogeochem. Cycles* **16**: 1107.
- Sett, S., L. T. Bach, K. G. Schulz, S. Koch-Klavsen, M. Lebrato, and U. Riebesell. 2014. Temperature modulates coccolithophorid sensitivity of growth, photosynthesis and calcification to increasing seawater pCO₂. *PLoS ONE* **9**: e88308 doi:[10.1371/journal.pone.0088308](https://doi.org/10.1371/journal.pone.0088308).
- Shutler, J., P. Land, C. Brown, H. Findlay, C. Donlon, M. Medland, R. Snooke, and J. Blackford. 2013. Coccolithophore surface distributions in the North Atlantic and their modulation of the air-sea flux of CO₂ from 10 years of satellite Earth observation data. *Biogeosciences* **10**: 2699–2709.
- Signorini, S. R., B. A. Franz, and C. R. McClain. 2015. Chlorophyll variability in the oligo-trophic gyres: Mechanisms, seasonality and trends. *Front. Mar. Sci.* **2**: 11.
- Sprengel, C., K.-H. Baumann, J. Henderiks, R. Henrich, and S. Neuer. 2002. Modern coccolithophore and carbonate sedimentation along a productivity gradient in the Canary Islands region: Seasonal export production and surface accumulation rates. *Deep-Sea Res. Pt. II* **49**: 3577–3598.
- Steinmetz, J. 1991, p. 41. *In* S. Honjo [ed.], *Calcareous nannoplankton biocoenosis: Sediment trap studies in the Equatorial Atlantic, Central Pacific, and Panama Basin*. Woods Hole Oceanographic Institution Woods Hole Massachusetts.
- Stuut, J.-B. W., and others. 2013. Cruise report and preliminary results (64PE378), TRAFFIC II: Transatlantic fluxes of Saharan dust (Las Palmas de Gran Canaria, Spain – St. Maarten). Royal NIOZ, p. 54.
- van der Does, M., G.-J. A. Brummer, F. C. J. van Crimpen, L. F. Korte, N. M. Mahowald, U. Merkel, and others. 2020. Tropical rains controlling deposition of Saharan dust across the North Atlantic Ocean. *Geophys. Res. Lett.* **47**: e2019GL086867. doi:<https://doi.org/10.1029/2019GL086867>
- van der Jagt, H., C. Friese, J.-B. W. Stuut, G. Fischer, and M. H. Iversen. 2018. The ballasting effect of Saharan dust deposition on aggregate dynamics and carbon export: Aggregation, settling, and scavenging potential of marine snow. *Limnol. Oceanogr.* **63**: 1386–1394. doi:<https://doi.org/10.1002/lno.10779>
- Waniek, J., W. Koeve, and R. D. Prien. 2000. Trajectories of sinking particles and the catchment areas above sediment traps in the Northeast Atlantic. *J. Mar. Res.* **58**: 983–1006.
- Young, J. R., and P. Ziveri. 2000. Calculation of coccolith volume and its use in calibration of carbonate flux estimates. *Deep-Sea Res. Pt. II* **47**: 1679–1700.
- Ziveri, P., A. Rutten, G. J. de Lange, J. Thomson, and C. Corselli. 2000. Present-day coccolith fluxes recorded in central eastern Mediterranean sediment traps and surface sediments. *Palaeogeogr. Palaeoclimatol. Palaeoecol.* **158**: 175–195.
- Ziveri, P., B. de Bernardi, K.-H. Baumann, H. M. Stoll, and P. G. Mortyn. 2007. Sinking of coccolith carbonate and potential contribution to organic carbon ballasting in the deep ocean. *Deep-Sea Res. Pt. II* **54**: 659–675.
- Zondervan, I. 2007. The effects of light, macronutrients, trace metals and CO₂ on the production of calcium carbonate and organic carbon in coccolithophores—A review. *Deep-Sea Res. Pt. II* **54**: 521–537.

Acknowledgments

The authors thank the crews of Meteor cruise M89, Pelagia cruise 64PE378, RV Poseidon cruises POS425, POS445 and POS464, as well as the NIOZ and MARUM technicians for their contributions. Moorings M4, M2, and M1 were managed by the NIOZ in the framework of the projects TRAFFIC funded by NWO (no. 822.01.008), and DUSTTRAFFIC funded by

ERC (no. 311152), directed by Jan-Berend W. Stuut. Moorings CB-23 and CB-24 were managed by Gerhard Fischer as part of the MARUM project GB1 (Particle flux, carbon turnover and nutrient regeneration). Lab preparation of the 1/5 split of the original sediment trap sample for M4, M2 and M1 was conducted at the NIOZ; the splitting, filtering, and SEM taxonomical analysis were performed at Uni-Bremen, Germany. The quantification and discussion of the coccolith-CaCO₃ fluxes were performed at MARUM, Germany, and at MARE/Uni-Lisbon, Portugal. The first author benefited from a Marie Skłodowska-Curie Fellowship supported by Uni-Bremen and the EU FP7 COFUND (grant no. 600411) and from a Marie Skłodowska-Curie European Fellowship supported by the EU H2020-MSCA-IF-2017 (grant no. 796802) within DUSTCO. Currently, the first author benefits from a research contract funded by FCT (contract CEECIND/00752/2018/CP1534/CT0011) linked to project CHASE (www.chase-dust.com). This study was also supported by PORTWIMS (<https://www.portwims.org>) funded by the EU's H2020 Research and Innovation Programme (grant no. 810139), iFADO from ERDF funds of the INTERREG

Atlantic Area Programme (contract EAPA-165/2016), CALMED (#CTM2016-79547-R) and the Generalitat de Catalunya MERS (#2017 SGR-1588). The authors acknowledge the NASA's Ocean Biology Processing Group (<https://oceancolor.gsfc.nasa.gov>), as well as the constructive suggestions and encouraging remarks by two anonymous reviewers and by the Editor-in-Chief Dr. K. David Hambright.

Conflict of Interest

None declared.

Submitted 05 August 2020

Revised 25 January 2021

Accepted 29 May 2021

Associate editor: Thomas R. Anderson